



## **DIPLOMARBEIT**

# Influences of varying oxygen, glucose, and lactate concentrations on the osteogenical development of adipose derived mesenchymal stem cells

ausgeführt zum Zwecke der Erlangung des akademischen Grades eines  
Diplom-Ingenieurs unter der Leitung von

**Professor Dr. Cornelia Kasper**

Institut für Angewandte Mikrobiologie der Universität für Bodenkultur Wien

eingereicht an der Technischen Universität Wien

**Fakultät für Maschinenwesen und Betriebswissenschaften**

von

**Daniel Remmers**

Matrikelnummer: e1128435  
Adresse: Leonrodstr. 89  
80636 München

Wien, im \_\_\_\_\_

## **Acknowledgements**

Ich danke Frau Prof. Dr. Cornelia Kasper für die Übernahme der Erstprüfung und die freundliche, zeitintensive Betreuung. Für die Übernahme der Zweitprüfung bin ich Herrn Prof. Dr. Christian Hellmich sehr verbunden.

Außerdem möchte ich herzlichst Verena Charwat für Ihre Hinwendung und ihre stets hilfreichen Ratschläge danken.

Weiters gilt mein Dank meiner Familie sowie Christa und Hans-Dieter Ulrich, für deren aufopfernde Fürsorge und Unterstützung während meiner akademische Ausbildung.

## Table of content

|  |     |
|--|-----|
| Abstract.....  | VII |
| 1 Introduction .....                                   | 1   |
| 2 Theoretical background .....                         | 3   |
| 2.1 Osteogenic differentiation .....                   | 3   |
| 2.2 Cellular respiration.....                          | 4   |
| 2.2.1 Aerobic respiration.....                         | 4   |
| 2.2.2 Lactic acid fermentation .....                   | 7   |
| 2.3 Lactate yield coefficient .....                    | 9   |
| 2.4 Metabolism under different conditions .....        | 11  |
| 2.4.1 Influences of hypoxic conditions .....           | 11  |
| 2.4.2 Influences of lactic acid .....                  | 15  |
| 2.4.3 Influences of lactate and osmotic pressure ..... | 18  |
| 2.5 Mechanosensation .....                             | 19  |
| 2.5.1 Mechanoreception.....                            | 19  |
| 2.5.2 Mechanotransduction .....                        | 20  |
| 3 Experimental design.....                             | 22  |
| 4 Results and discussion.....                          | 23  |
| 4.1 Staining analysis .....                            | 23  |
| 4.2 Microscopical analysis .....                       | 31  |

|       |  |    |
|-------|--|----|
| 4.2.1 | DAPI and calcein fluorescence analysis .....         | 31 |
| 4.2.2 | Light microscopy and morphological analysis .....    | 34 |
| 4.2.3 | Microscopic non-average findings .....               | 43 |
| 4.3   | Glucose consumption, lactate production and LYR..... | 45 |
| 4.4   | Mechanical promotion of osteogenesis.....            | 55 |
| 5     | Summary and conclusion .....                         | 57 |
| 6     | Appendix .....                                       | 59 |
|       | Materials .....                                      | 59 |
|       | Media .....  | 63 |
|       | Cell culture .....                                   | 64 |
|       | Adipose tissue derived stem cells.....               | 64 |
|       | Handling .....                                       | 64 |
|       | MSC donors .....                                     | 66 |
|       | Histological examination and measurements .....      | 67 |
|       | Publication bibliography .....                       | 77 |

## List of abbreviations

|        |  |
|--------|--|
| adMSC  | adipose derived mesenchymal stem cell                        |
| ADP    | adenosine diphosphate  |
| ATP    | adenosine triphosphate                                       |
| Ca     | calcium  |
| DMEM   | Dulbecco's modified eagle's medium                           |
| DNA    | desoxyribonucleic acid                                       |
| ECM    | extracellular matrix   |
| HIF    | hypoxic induced factor – 1a                                  |
| LYR    | lactate yield ratio  |
| MSC    | mesenchymal stem cell  |
| MTT    | 3-(4,5-dimethylthiazol-2-yl)-2,5-diphenyltetrazolium-bromide |
| NAD    | nicotine amide dinucleotide                                  |
| NADH   | nicotinamide adenine dinucleotide H                          |
| NaLLA  | sodium L-lactate   |
| NaOH   | sodium hydroxide   |
| PDC    | pyruvate dehydrogenase complex                               |
| ROS    | reactive oxygen species                                      |
| RT-PCR | reverse transcription polymerase chain reaction              |

## Figure table

|  |    |
|--|----|
| Figure 1: Chemical pathway from glucose over glycolysis to the citric acid cycle .....   | 6  |
| Figure 2: Citrate molecule.....  | 7  |
| Figure 3: Oxidation of pyruvate to lactate involving NADH .....  | 8  |
| Figure 4: Citric acid cycle including the insertion site of glutamine .....  | 10 |
| Figure 5: L-lactic acid.....   | 15 |
| Figure 6: Representative wells after staining .....  | 24 |
| Figure 7: Cultivation plates after staining.....   | 25 |
| Figure 8: Quantity of staining intensities of cell layers on differentiation day 7 and 12 regarding cell culture conditions..... | 28 |
| Figure 9: Fluorescence microscopy after incubation with DAPI and calcein solution. ....  | 33 |
| Figure 10: Light microscopy after alizarin red and von Kossa staining....  | 35 |
| Figure 11: Fluorescence microscopy after incubation in DAPI and calcein solution – different from the norm. ....                 | 36 |
| Figure 12: Light microscopic pictures after alizarin red and von Kossa staining – different from the norm .....                  | 38 |
| Figure 13: Light microscopic pictures .....  | 40 |
| Figure 14: Proliferation and ECM development during ossification .....   | 42 |
| Figure 15: Microscopical peculiarities of fluorescence and light-microscopic shots structured in a pairwise manner .....         | 43 |

|  |    |
|--|----|
| Figure 16: Averaged daily values of lactate production, glucose consumption and lactate yield coefficient over the differentiation period of 12 days ..... | 46 |
| Figure 17: Average glucose and lactate concentration over time .....   | 49 |
| Figure 18: Standard deviations and coefficients of variations for lactate for DMEM (A) and $\alpha$ MEM (B) regarding the absolute values .....            | 51 |
| Figure 19: Standard deviations and coefficients of variations for glucose for DMEM (A) and $\alpha$ MEM (B) regarding the absolute values .....            | 51 |
| Figure 20: Standard deviations and coefficients of variations for lactate for DMEM (A) and $\alpha$ MEM (B) regarding the daily changes.....               | 53 |
| Figure 21: Standard deviations and coefficients of variations for glucose for DMEM (A) and $\alpha$ MEM (B) regarding the daily changes .....              | 53 |
| Figure 22: Daily values for glucose, lactate and LYR.....  | 54 |
| Figure 24: Error curve for glucose showing the differences between real and measured values .....  | 69 |
| Figure 25: Error curve for lactate showing differences between real and measured values .....  | 70 |

---

## **Abstract**

---

The aim of this work is to investigate the impact of varying cell culture conditions on the osteogenic differentiation of adMSCs. Glucose and oxygen supply are two parameters which are known for their strong impact on cell behavior. Therefore, the effect of glucose and atmospheric oxygen concentration are examined in this study individually and in combination.

Cells are cultivated over a period of 12 days under either high (21%) or low (5%) atmospheric oxygen concentrations and in osteogenic differentiation media with high (4%) or low (1%) glucose concentration. Medium change is carried out in a batch-process approach: A complete medium change is performed every three days to replenish glucose as well as other nutrients and growth factors and to remove lactate and other waste products. Daily measurements of glucose and lactate are performed to compare metabolic activity of the cells under the different cultivation conditions. Special focus is put on discriminating between the effects of glucose concentration and the metabolic changes in response to rising lactate levels. Differentiation is monitored by staining for ECM mineralization: Alizarin red and calcein staining are performed to detect calcification, while phosphate deposition is visualized by von Kossa staining. Cell load and cell distribution are shown by DAPI fluorescence staining of cell nuclei.

Results of the study show glucose restriction in the presence of the low-glucose medium. Based on staining results for normoxia experiencing adMSCs, low- and high-glucose media lead to comparable results concerning the osteogenic differentiation. Regarding oxygen availability normoxic (21% oxygen) conditions result in lower glucose consumption rates and a stronger and earlier ECM ossification compared to atmospheric conditions of 5% oxygen. Alizarin red staining significantly detects ECM

calcification as early as on differentiation day 7 when cultured under normoxic conditions. This behavior is observed for young (passage zero) adMSCs and passage number of the donor cells could be a crucial impact on the cell response to normoxic and hypoxic conditions. Generally, earlier and stronger mineralization is observed close to the border of the cell culture vessel. The study also shows a correlation between low lactate yield ratios and strong osteogenic differentiation.

---

## **1 Introduction**

---

Due to the rising demand for organ transplants, autogenic tissues or the use of injected progenitor cells to support the treatment of cancer, research on stem cells and their potential benefit in healthcare gains more and more recognition. Transplant organs experience rejection reactions as its cells don't originate from the recipient. With the use of adult human stem cells like homologous mesenchymal stem cells, rejection reactions can be avoided. One major aspect of this research is the cultivation of stem cells with the ability to differentiate osteogenically into bone tissues. By the use of these progenitor cells, besides other possible benefits, bones with complicated fractures could be restored more frequently and with less effort. Although great progression was achieved recently, state of the art culture conditions for this purpose possess potential for improvement.

Therefore, this work analyzes the influence of physical parameters that might have a positive impact on growth and osteogenic differentiation of mesenchymal stem cells. Important parameters for the growth and differentiation are concentrations of oxygen, glucose and its metabolite lactate.

To gain further insights on the impact of these parameters mesenchymal stem cells are cultured over a twelve-day investigation period in low- and high-glucose differentiation medium under normoxic and hypoxic atmosphere conditions with 21 and 5 % oxygen. Measurements of glucose and lactate are conducted on a daily basis to analyze the correlation between their concentrations and the progression in differentiation. Also a morphological examination based on the operated light microscopy is conducted. DAPI- and calcein-fluorescence microscopy assays are performed as well as alizarin red and von Kossa staining to monitor the ossification status.

The results and the further interpretation shall be based on the current theoretical knowledge on this topic. Therefore chapter 2 contains the theoretical background. Subject matter of this chapter is varying forms of cellular respiration and their impact on osteogenic differentiation. Additionally, effects of mechanical stimuli as well as glucose and lactate concentrations are taken into consideration. Chapter 3 precisely describes the experimental design whereas chapter 4 comprises observations and results originating from glucose and lactate measurements, staining analyzes and light and fluorescence microscopy. The terminal chapter, chapter 5, provides a general conclusion based on the findings.

---

## **2 Theoretical background**

---

### **2.1 Osteogenic differentiation**

Bone formation appears when the so called osteoblasts secrete osteoid. Osteoid is an unmineralized bone matrix occurring in early stages of bone formation. It mineralizes successively over time and consists of 90 % type I collagen to build up fibrils and 10 % of other non-collagenous proteins such as osteocalcin, osteonectin and osteopontin. The physiological mineralization of osteoid needs approximately 3-6 months per unit to finalize in the human body. A level of approximately 70% is achieved after 5-10 days. The bone mineral is formed from mainly impure tricalcium phosphate, more precisely carbonated hydroxyapatite ( $\text{Ca}_{10}(\text{PO}_4)_6(\text{OH})_2$ ). Osteoblasts ensure growth, repair and adaption of bones to changing mechanical demands. Furthermore, they participate in the calcification, bone resorption and calcium-/ phosphate flux processes. Osteoblasts arise from mesenchymal stem cells that are capable of the osteogenic lineage differentiation. Naturally osteoblasts are located near the periosteum and endosteum or the marrow stroma (Cowin 2001).

To initiate in vitro development of adMSCs towards the osteogenic lineage the scientific standard procedure is to add dexamethasone, L-ascorbic acid and beta glycerophosphate. While dexamethasone initializes osteogenic differentiation by up-regulation of Runx2 activity, ascorbic acid leads toward a raised collagen I production and collagen-I integrin-mediated intracellular signaling. Beta glycerophosphate serves by supplying a phosphate source for the formation of hydroxyapatite (Langenbach, Handschel 2013). The osteogenic differentiation is initiated by a phase of increased proliferation (Aubin, Triffitt 2002). Although more recent studies suggest a minimum of seven distinct differentiation stages, the three main and well characterized stages are proliferation, matrix maturational phase

and mineralization. In addition to the extrinsic factors dexamethasone, glycerophosphate and ascorbic acid, intrinsic conditions such as cell-cell contacts and extracellular matrix conditions play an important role. Hyaluronic acid has been shown to effect embryonic stem cells due to maintenance of the pluripotent state. Furthermore, proteins of the ECM (extracellular matrix) such as collagen and fibronectin influence the osteogenic initialization of MSCs. (Coan, Heather Adeline Bradbury 2011). The literature has shown that the differentiation of MSCs that secrete preliminary ECM influences surrounding MSCs (Xu et al. 2009; Hoshiba et al. 2009). One study that cultivated adMSCs in ECM-coated culture dishes from an earlier MSC differentiation showed higher calcification on day 16 compared to a cultivation in non-coated dishes on day 30 (Coan, Heather Adeline Bradbury 2011). In another study performed by Müller *et al.* mineralization was monitored as early as on differentiation day 8 (Müller et al. 2008). In these studies differentiation was induced using the same osteogenic additives that are utilized in the work on hand.

## **2.2 Cellular respiration**

The following describes the chronology, possibilities and metabolic pathways of the eukaryotic adMSCs to gain energy e.g. by utilizing glucose in an exothermic redox reaction. The cellular respiration can be distinguished in aerobic respiration and anaerobic respiration.

### **2.2.1 Aerobic respiration**

Aerobic respiration can be claimed to be the most important respiratory pathway. Under perfect conditions the overall outcome of aerobic respiration can be stated as 38 ATP molecules per molecule glucose. Due to losses (e.g. leaky membranes and migrating pyruvate and ADP into the

mitochondrial matrix) estimations range around 29 to 30 ATP per molecule glucose for the overall outcome (Poor 2003).

The aerobic respiration can be separated into four sections, as there are glycolysis, oxidative decarboxylation of pyruvate, citric acid cycle and the oxidative phosphorylation. The process of glycolysis which can be seen in Figure 1 takes place in the cytosol of the cell in both, the aerobic and in the anaerobic respiration. Glucose gets phosphorylated to fructose 1,6-biphosphat via two molecules ATP and the intermediate step glucose 1,6-biphosphate. The produced double phosphorylated compound splits into two phosphorylated molecules that later degrade into pyruvate. After deductions glycolysis emits two molecules ATP, 2 NADH, 2 pyruvate, 2 H<sup>+</sup> and 2 H<sub>2</sub>O plus heat.

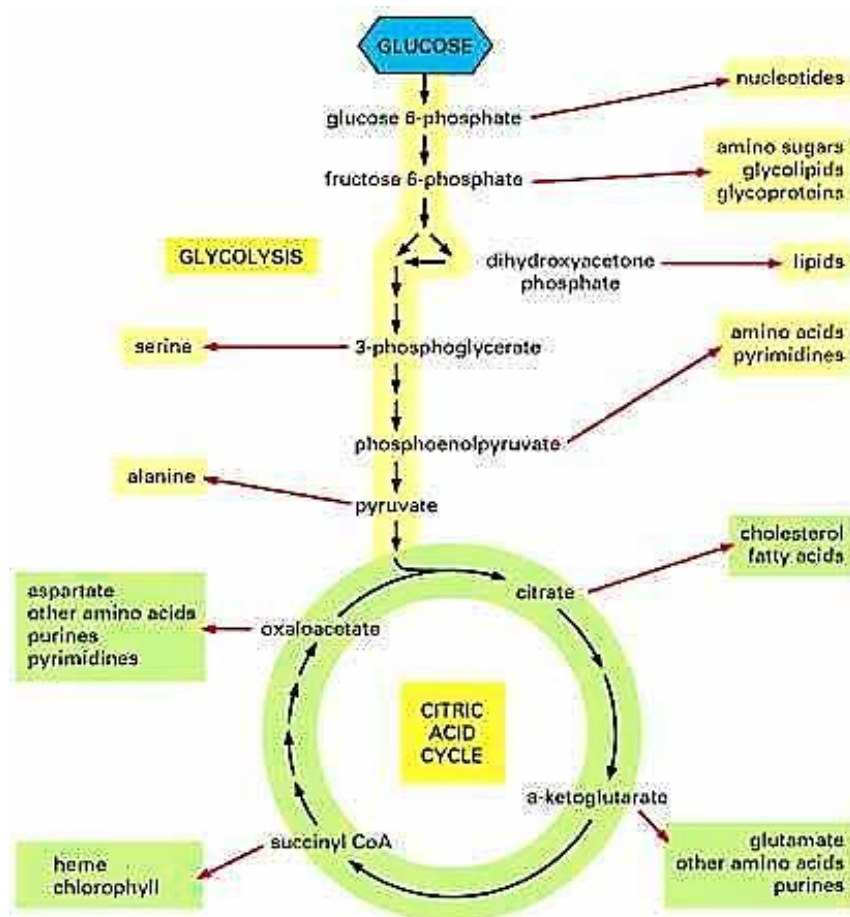


**Figure 1: Chemical pathway from glucose over glycolysis to the citric acid cycle**

Under aerobic conditions the produced pyruvate is transported to the inner mitochondria membrane where oxidative decarboxylation takes place. The pyruvate dehydrogenase complex (PDC) oxidizes pyruvate to acetyl-CoA and  $\text{CO}_2$  while transmitting the acetyl-group to coenzyme A (CoA). One molecule pyruvate results in one molecule NADH, acetyl CoA and  $\text{CO}_2$ .

Krebs cycle also known as citric acid cycle follows the acetyl CoA production under aerobic conditions. Here, acetyl CoA is oxidized to  $\text{CO}_2$  while reducing  $\text{NAD}^+$  to NADH. The Krebs cycle consists of 8 steps driven by different enzymes and co-enzymes. In the beginning of the cycle acetyl CoA is being condensed with oxaloacetate to citrate ( $\text{C}_6\text{H}_8\text{O}_7$ ); rearranged and after cleaving of  $\text{CO}_2$  and several further steps oxaloacetate appears

again. The two entering acetyl CoA molecules result in 6 NADH, 2 FADH<sub>2</sub>, 2 GTP, 4 CO<sub>2</sub>, 4 H<sub>2</sub> und 2 coenzymes A.

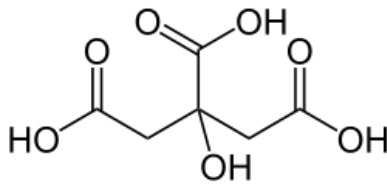


**Figure 2: Citrate molecule**

NADH molecules produced in the beginning of the Krebs cycle can be used by the mitochondrial cristae in the electron transport chain to establish a proton gradient across the inner mitochondrial membrane. The effect is a chemiosmotic potential that is used to drive the oxidative phosphorylation of ADP - by means of ATP synthase - by pumping protons from the inter-membrane chamber back to the mitochondrial matrix. At the end of the electron transport chain two protons derived from hydrogen are transferred to oxygen. The waste products of the described process are H<sub>2</sub>O and CO<sub>2</sub>.

### **2.2.2 Lactic acid fermentation**

The lactic acid fermentation is an anaerobic fermentation reaction and consists of the glycolysis with a subsequently oxidation of pyruvate to lactate by means of lactate dehydrogenase. Here NADH - an energy transferring compound that had been produced in the former pyruvate production - is oxidized to NAD<sup>+</sup>. This reaction with its outcome of 2 ATP molecules in total is less efficient compared to the cellular aerobic respiration with a net outcome of approximately 30 ATP (Poor 2003). The reaction velocity of the lactic acid fermentation is a major advantage. Lactate, the waste product of the lactic acid fermentation is being

produced in mammalian muscles during high energy demands. Normally mammalian cells mainly undergo cellular respiration in the presence of sufficient oxygen concentrations. Nevertheless, lactic acid fermentation can occur under aerobic conditions. In the end of this metabolic pathway, one glucose molecule affects in two molecules of lactic acid. After dissolution and protolysation, the remaining lactate group forms an ionic bond together with sodium ions ( $\text{Na}^+$ ) or potassium ions ( $\text{K}^+$ ) resulting in the salt lactate.

Lactate was considered a waste product which cannot be used metabolically as an energy containing compound. Meanwhile it is common knowledge that lactate can be restored to pyruvate through a process known as the cori cycle. Transported to the liver, lactate can be re-transformed to pyruvate in the presence of oxygen, which can then be converted into glucose (Abbiss, Laursen 2005).

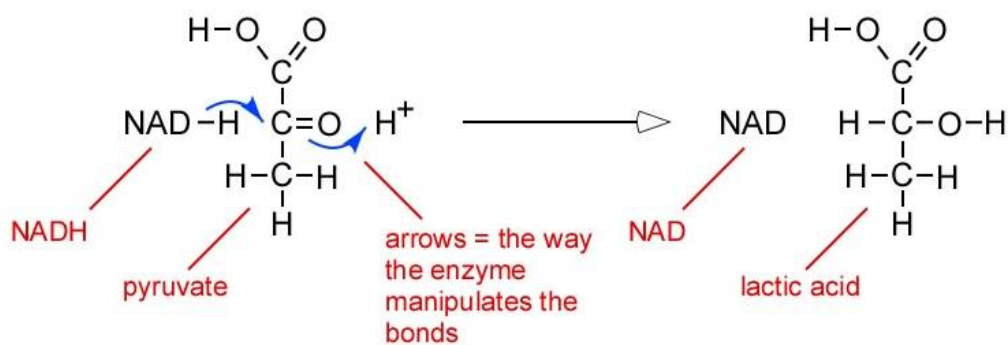


**Figure 3: Oxidation of pyruvate to lactate involving NADH**

### **2.3 Lactate yield coefficient**

Even if the supply of oxygen is sufficient, cells undergo the lactic acid fermentation in a certain ratio (Deschepper et al. 2011; Krebs 1972), this behavior is known as the Warburg effect. With the aid of the lactate yield coefficient that is the molar ratio of lactate production to glucose consumption, a statement can be made concerning the percentage of aerobic respiration the cell cultures undergo. Additionally, varying lactate yield coefficients can indicate a major metabolic shift.

As mentioned in the previous section, multipotent cells tend to prefer lactic acid fermentation in order to prevent DNA impairment that is accompanied with an increase of the lactate yield coefficient. Grayson *et al.* were able to proof a shift in the lactate yield coefficient when cell cultures under different oxygen conditions were compared. Cultivation under hypoxic conditions of 2% O<sub>2</sub> led to an average final LYR of 2.5 compared to 1.7 under normoxic conditions (Grayson et al. 2006).

#### **LYRs exceeding the value of two**

When sugars are supposed to be the only high energetic carbon source entering the citric acid cycle, lactate yield ratios above 2 could not be reached. As Borle *et al.* gained rising lactate concentrations in the absence of glucose, other energy supplying molecules entering the glycolysis have to be present in order to explain this result (Borle et al. 1960). Although one glucose molecule does effect in two lactate molecules tops, physiological lactate yield ratios exceeding values of 2 can occur naturally. As other compounds besides sugar, like L-glutamine are also transformed to lactic acid, ratios higher than 2 do not imply a failed application. During glycolysis sugar is cleaved into 2 molecules of lactate. Amino acids contribute to cellular energy metabolism by providing a carbon source for the citric acid cycle (tricarboxylic acid cycle). This is especially the case when a primary source of energy, such as glucose, is scarce or when cells

undergo metabolic stress (McCall et al. 1982). A special quality of L-glutamine that is present in the used cell culture media alpha and DMEM, is the ability of mitochondria to utilize and transform glutamine into lactate. The transformation of other amino acids into lactate is a quality that is physiologically possible in the human body but needs assistance of the liver. Relatively high L-Glutamine concentrations present in cell cultivation media can be a major reason for lactate yield ratios exceeding LYRs (Ozturk et al. 1992; Hevehan, De Bernardez Clark, Eliana 1997). L-glutamine provides nitrogen for NAD, NADPH and nucleotides and serves as a secondary energy source for metabolism. During the metabolic pathway from glutamine to lactate, a process called glutaminolysis, presented in Figure 4, takes place. Here glutamine is cleaved successively into glutamate, aspartate, CO<sub>2</sub>, pyruvate and eventually into lactate (MCKEEHAN 1982; Krebs, Bellamy 1960).

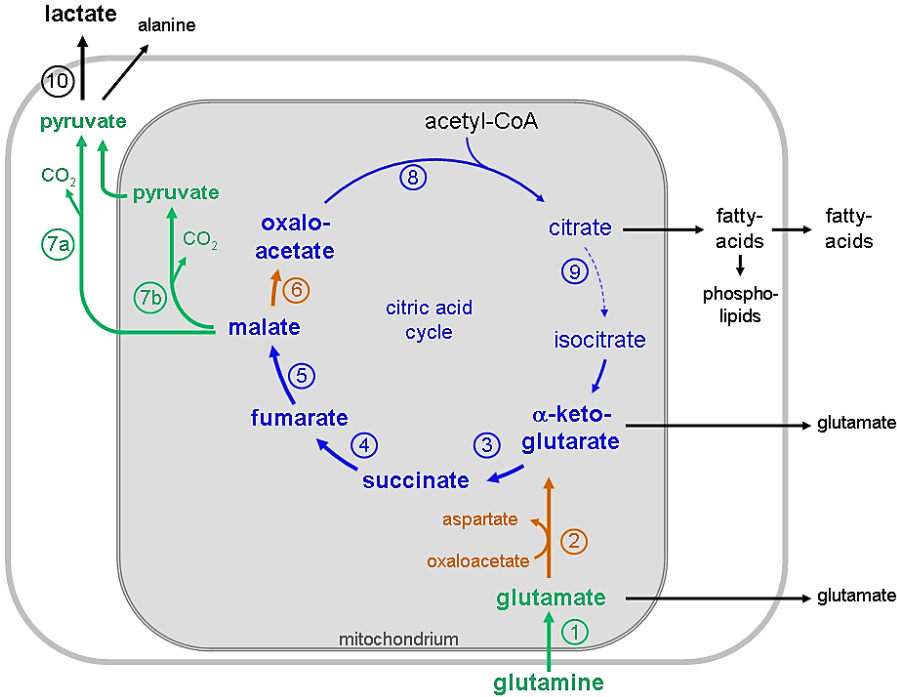


**Figure 4: Citric acid cycle including the insertion site of glutamine; source: Sybille Mazurek**

Human blood serum, used for the thesis on hand, contains chemical compounds like fatty acids, glutamine and sugars. Sugars, glutamate and

glutamine can be used as an energy source leading to an additional pyruvate or potential lactate supply and therefore raising LYRs. The average glutamine and glutamate values range from 600-800 and 30-70  $\mu\text{mol/L}$  (*equates with 8.77-11.69 and 0.44-1.02 mg/dL*) in blood plasma (FELIG et al. 1970). Sugar concentrations of adults such as glucose or fructose in the blood plasma range from 7 to 10.5 mg/dL and 7-8 mg/dL. As serum makes up to 10 % of the culture media, the basal sugar concentration is raised by approximately 2 mg/dL from sugar only. The glucose concentrations in the used culture media range from 100 mg/dL in  $\alpha$ MEM to 450 mg/dL in DMEM. L-Glutamine ranges from 29.2 mg/dL in  $\alpha$ MEM and 58.4 mg/dL in DMEM. Pyruvic Acid is contained within these cell culture media with concentrations up to 11 mg/dL. The present glutamine and glucose and pyruvate in the cell culture media together with the serum immanent concentrations of both compounds add up to values possibly exceeding 40 mg/dL (Weatherby, Ferguson 2004). These sources result in a raise of potential metabolic lactate educts of about 40 % in the case of  $\alpha$ MEM and 10 % for DMEM.

## **2.4 Metabolism under different conditions**

Metabolic behavior of cells is dependent on the conditions the cells experience. To examine these conditions and their effects on the cells metabolism is the purpose of the following chapters.

### **2.4.1 Influences of hypoxic conditions**

When mammalian cells are cultivated under hypoxic oxygen conditions a metabolic change towards a higher glucose consumption mechanism takes place (Guillemin, Krasnow 1997; Malhotra, Brosius 1999). This is caused by the transcription factor HIF-1a (Hypoxic induced factor - 1a). Seagroves *et al.* showed that HIF-1a regulates the metabolic change by

adjusting the glucose consumption to a higher level and therefore, overcoming the less efficient lactic acid fermentation metabolism (Seagroves et al. 2001).

#### **2.4.1.1 Influences on stem cell cultivation under hypoxic conditions**

Cell culture gains good results by mimicking the natural physiological conditions. Therefore, cultivation under physiological oxygen conditions should be considered. The average physiological oxygen concentration in the human tissue is 3% (Csete 2005), while the well blood supplied bone marrow provides oxygen concentration of 5 % (Hevehan et al. 2000).

Human MSCs are able to survive in extremely hypoxic environments e.g. by adaption and persisting in a quiescent state using glycolytic pathways (Cipolleschi et al. 1993). Grayson et al. were able to enlarge the proliferation rate under the use of a 3 % O<sub>2</sub> enriched atmosphere thirtyfold (Grayson et al. 2007). Concerning differentiation potential the scientific community came to differing conclusions so far. Oxygen conditions were testified to have an immanent effect on stem cell development. Beginning with concentration differences of 1-2 % O<sub>2</sub>, several partially diverging effects have been observed influencing stem cell development (Abdollahi et al. 2011). Stem cells - e.g. of the nervous system - tend to develop into various forms of nervous tissue cells under different oxygen conditions. Besides that, low oxygen cultivations showed to have less apoptotic tendencies (Studer et al. 2000). Hypoxia not only facilitates MSC expansion as described above, but also allows retaining stem-cell characteristics indicating a biological selection due to oxygen deprivation of more primitive cell stadiums. It was shown that the potential to maintain a dedifferentiated character is improved by lower oxygen levels (Ezashi et al. 2005; Prasad et al. 2009). Oxygen environments of 2% led to a significantly higher colony forming capability

and higher stem-cell-gene expression. A high colony forming potential is assumed to occur more likely in dedifferentiated cells than in less differentiated cells (Chen et al. 2009). Culturing hematopoietic stem or progenitor cells at different oxygen concentrations revealed that lower oxygen tensions, e.g. 1% O<sub>2</sub>, maintained the earliest progenitor cells (Cipolleschi et al. 1993). Osteogenic MSC development gained several partially differing results for hypoxic conditions in terms of suppressing versus stimulating osteogenic differentiation. D'Ippolito *et al.* found that low oxygen supply tends to suppress the osteogenic differentiation but increases the proliferation rate of bone marrow derived MSCs using dexamethasone, ascorbic acid and glycerophosphate. The mentioned study was conducted with different oxygen levels of 1, 3, 5, 10 and 21 %. Every sample cultivated in hypoxic conditions resulted in a higher proliferation rate compared to normoxic cultivations. For 3% O<sub>2</sub> the proliferation rate increased by nearly 120% in average. But the ossification of the cells was suppressed resulting in a low calcium accumulation and ALP activity during a period of 15 days (D'Ippolito et al. 2006). Tests on osteogenic differentiation were, other than tests on proliferation, performed under one single oxygen concentration (3% O<sub>2</sub>). D'Ippolito *et al.* are suggesting that low oxygen tension has a suppressing effect on osteogenic differentiation. This study was conducted on cell passages 1 to 6.

#### **2.4.1.2 Niche theory concerning stem cells**

Brand *et al.* showed that silent T-lymphocytes use the metabolic pathway of the aerobic respiration in comparison to the lactic acid fermentation with a ratio of 80 % in normal steady phases, but undergo the same pathway with a ratio of 14 % during proliferation (Brand, Hermfisse 1997). One reason causing this cellular behavior in the case of stem cells is the need to abandon reactive oxygen species (ROS) that harm the cell as a whole, their protein and lipid structure and especially the DNA (Keith,

Simon 2007). Lactic acid fermentation is less efficient compared to aerobic respiration. A big advantage it offers, is that by its use ROSs can be avoided (Poor 2003). As MSCs that are capable of a high number of cell divisions are crucial for the body's health state, the abandonment of DNA endangerments like ROSs is indispensable, causing proliferating MSCs to prioritize lactic acid fermentation over aerobic respiration even under sufficient oxygen conditions. To explain higher stem cell appearance in low oxygen regions and the ability of decreased oxygen levels to maintain a dedifferentiated stem cell stage, D'Ippolito *et al.* hypothesize a setting in which mesenchymal stem cells live in biological niches during extreme low oxygen supply phases. (D'Ippolito *et al.* 2006). As a result DNA is protected during low oxygen phases when the stem cell potential is less needed.

#### **2.4.1.3 Time-dependent hypoxia**

Studies by Basciano *et al.* revealed a long term advantage of hypoxic conditions in terms of proliferation and differentiation. MSCs were cultivated in hypoxia as well as in normoxia and with the start of passage two translated into osteogenic lineage specific medium. Hypoxic cultivated MSCs of passage zero were compared to cells at passage two in hypoxia and normoxia. In hypoxia, cells gained fewer and smaller colonies. An inhibition of genes involved in DNA metabolism and cell cycle progression was observed. Hypoxia maintained the cells morphologically undifferentiated. Hypoxic MSCs contained less mitochondria. After a lag phase, cells at passage 2 in hypoxia outgrew cells cultured in normoxia and showed higher production rates of genes involved in extracellular matrix assembly (4-60-fold). Histological staining and RT-PCR (Reverse transcription polymerase chain reaction) were performed for the amplification of osteocyte lineage-specific transcripts (ALPL, Runx2). ALPL showed a higher expression in hypoxic MSCs. While Runx2 transcription was undetectable in normoxia, hypoxia induced Runx2 expression.

Furthermore, hypoxia generated approximately 50% more osteogenic colonies compared to normoxia. These results suggest that hypoxia enhanced a genetic program that maintained the cells multipotent character. The duration of hypoxic conditions may play a crucial role concerning the differentiation potential of MSCs toward the osteogenic lineage (Basciano et al. 2011).

#### **2.4.2 Influences of lactic acid**

For the following analysis the transition of lactic acid into lactate is taken into consideration. Under common physiological conditions lactic acid quickly transforms to lactate in the human body. As the bigger residuum of lactic acid after the dissolution is bound in an ionic bond and therefore not available for the reunion with the hydrogen ion, nearly every lactic acid molecule will be existent in the form of lactate when not present in an extreme acidic environment. This tendency to deprotonate is the consequence of the intramolecular hydrogen bridge between the  $\alpha$ -hydroxyl and the carboxylate group, making the carboxylate group less capable of strongly attracting its proton (Dawson 1959). Therefore, besides lactic acid and its impact on pH values, major attention of the work on hand is paid to the effects of lactate concentrations.

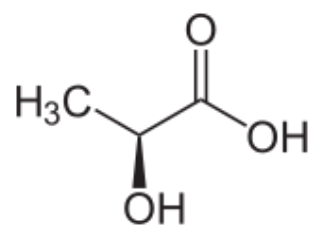


**Figure 5: L-lactic acid**

2013 He *et al.* undertook a study with rat bone marrow derived MSCs in which they analyzed the cytotoxicity of L-lactic acid during osteogenic differentiation on ossification and viability. Using a MTT assay and alkaline phosphatase (ALP) staining, the negative pH-decreasing impact on viability rates and ossification velocity was revealed (He et al. 2013).

Other studies proved decreased pH values to negatively influence cell proliferation as well (Patel et al. 2000; Kaysinger, Ramp 1998). The desired pH value for cell cultivation is between 7 and 7.4. The study was conducted with low-glucose and high-glucose Dulbecco's modified Eagle's medium (DMEM). The different media content did not affect the pH value of the media. With the aid of sodium hydroxide (NaOH), and sodium L-lactate (NaLLA) groups a decoupling analysis was performed to distinguish between the effects of lactate group accumulation and ion strength increase from the mechanisms of medium pH decrease. Hence this analysis, one could testify suppressing effects of pH decreases and the beneficial effects of a minor alkaline environment for cell viability (He et al. 2013).

Adapting the definition of the standard RGR (GB/T 16886.5-2003) (Chen et al. 2009), tolerated concentrations of L-lactic acid for rat MSCs are between 20-40 mmol;  $180.18 - 360.36 \text{ mg/dL}$  (Dawson 1959). An examination of the effects of 40 mmol/L resulted in a decrease of alkaline phosphatase activity of more than 50 % relative to the blank control. Alkaline phosphatase is responsible for the cleavage of phosphate groups and needed for the deposition of minerals in the ECM. Lactic acid concentrations of 40 mmol/L led to medium pH values of approximately 5, whereas concentrations of 20 mmol/L affected in values of approximately 6.5.

Studies stating suppressing effects of increased lactate concentrations were performed by several scientific units (Lao, Toth 1997; Omasa et al. 1992; Hassell et al. 1991). A study conducted by Patel *et al.* in 2001 showed an ceasing effect on the proliferation potential in hematopoietic cell cultures when lactate concentrations exceeded 20 mmol (Patel et al. 2000).

Another study verifies lactic acid and lactate to suppress proliferation, metabolism and osteogenic differentiation capacity of rabbit mesenchymal stem cells during cultivation in osteogenic medium. Several tests with sodium chloride and sodium hydroxide were performed to distinguish between effects of osmolarity, pH, and the chemical reaction potential and the osmotic pressure on the ossification potential due to higher concentrations of lactate ions. Concerning ossification inhibition tendencies, a decline in pH using NaOH had higher inhibition effects than lactic acid. Less negative tendencies were observed by the adjusted osmotic pressure, followed by lactate influences. As a conclusion the ossification inhibition is primary caused by the pH decreasing effect and secondly due to the lactate ion group and its osmolarity changing behavior. In the same examination, samples of fresh media with initial lactic acid and lactate concentrations of 5, 10 and 15 mmol/L (*equates with 45.05, 90.1 and 135.14mg/dL*) were produced and compared to a blank. Measured values were proliferation, colony-forming efficiency, ALP activity and calcium content after 11 days of cultivation. The results showed suppressing effects of the named additives proportional to their amount. Exceptional from this claim are the osmotic pressure adjustment and the additional 5mmol lactate - resulting in pH values of 7.20 – 7.40 - showing non-statistically significant differences compared to blank samples (Chen et al. 2009).

An increased lactate production can be observed for chondrogenic medium cultivation of MSCs under hypoxic conditions of 5% O<sub>2</sub> (Wang et al. 2005).

Interestingly, lipid accumulation was slightly but significantly ( $p < 0.05$  using a two-tailed t test) increased with rising lactate ion concentration. These adipogenic differentiation tendencies have also been observed due to decreasing pH ( $p < 0.05$ ). As lactic acid was shown to induce chondrogenic differentiation of dermal fibroblasts, one has to suggest that

lactic acid or its metabolites has an autocrine or paracrine effect on cellular differentiation (Nicoll et al. 2001).

### **2.4.3 Influences of lactate and osmotic pressure**

Varying lactate yield coefficients can indicate a major metabolic shift for instance in response to high concentrations of lactate (Ozturk et al. 1992; Lao, Toth 1997). This might be due to a lactate dehydrogenase inhibition. Lactate dehydrogenase reduces pyruvate producing lactate by consuming NADH (described in the chapter [Lactic acid fermentation](#)). Lactate dehydrogenase has been reported to be inactivated by exceeding lactate levels, resulting in a minor lactate production and therefore reduced lactate yield coefficients (Omasa et al. 1992). This adaption is a form of the balancing negative feedback mechanism.

Increasing LYRs might also originate in response to high osmotic pressures that lead to an increase in cell volume (Ozturk, Palsson 1991). Also a response of intracellular pH to increasing osmotic pressure might be a possible explanation (Ozturk et al. 1992).

## **2.5 Mechanosensation**

Concerning mechanosensation the question comes up how bone tissue and its precursors experience their demands in terms of mechanical strain (mechanoreception) and how this information is transmitted to other cells in the bone to start the signaling cascade that eventually leads to the formation of new bony material (mechanotransduction).

### **2.5.1 Mechanoreception**

Entrapped osteoblasts are called osteocytes. A network of these osteocytes, located in the bone, was widely suspected to be responsible for the mechanoreception during the last decades. Today this claim seems to be verified. The mentioned osteocytes exist in the so called lacunar-canalicular system, a three-dimensional tubular frame matrix, nerving the bone.

Although it is not yet entirely understood how osteocytes sense mechanical loads and initialize and orchestrate the following structural adaption, it is known that loading of the bone leads to a interstitial fluid flow through the unmineralized pericellular matrix that surrounds the osteocytes (Weinbaum et al.). This flow, respectively its impact, is assumed to be one of the main causes for the activation of osteocytes autocrine and paracrine stimuli excretion, that influences the metabolism of osteoblasts and osteoclasts (Xiong J. et al. 2011). Considering osteocytes to be responsible for the sensing of mechanical loading, several potential mechanisms have been suspected. These mechanisms include hydrostatic pressure, whole tissue strain, shear stresses, streaming potential and pulsatile flows of the bone fluid.

The assumption favoring shear stresses had formerly been very popular. To understand the source of shear stresses one has to know that loading of bones induces pressure gradients leading to a liquid shift of the

interstitial fluid while passing the lacunar-canalicular system. Interestingly not only the overall strain or load that is being put on the bone is relevant for a cellular bone adaption response, but also the frequency has an influence (Xie et al. 2006). According to current research even a cyclic hydraulic pressure of 68 kPa is sufficient in modulating signaling molecules transducing the demand for adaption in the osteocyte mouse cell-line MLO-Y4 which is often used for osteocyte researching purposes (Liu et al. 2010). This behavior might be an indicator for the importance of fluid flow as the frequency has an impact on the overall flow rate. Current studies show that interstitial fluid flow acts as a regulator of the metabolism of bony tissue and osteocytes in particular (Fritton, Weinbaum 2009).

Physiological loading causes strains in situ in a range of 0.04-0.3 % (Fritton et al. 2000). This range has been shown to neither stimulate osteocytes nor osteoblasts (You et al. 2000). Nevertheless, recent evidence shows that osteocytes may be excited by strains due to amplifications of the local strain via ultra-structural features inside and around osteocyte processes (Wang et al. 2007) or via strain concentrations occurring at lacunae (Nicolella et al. 2006) or bone remodeling units (McNamara et al. 2006).

### **2.5.2 Mechanotransduction**

When the mechanical loading exceeds or falls below threshold values a biochemical signaling reaction is induced within the osteocytes. This information needs to be transported to osteoblasts, bone lining cells and osteoclasts (Cowin, Doty 2007). Despite the recent efforts being made it is yet not clear how mechanical forces in the bone translate to chemical signals and coherently work together with other molecules involving signaling cascades in time- and rate-of-force-dependent manners (Vogel, Sheetz 2006). Four major possible mechanisms of detecting and transduction can be seen in ion channels (1), integrins and the

cytoskeleton (2), gap junctions and hemichannels (3) and primary cilia (4). Ion channels have an influence on osteocytes concerning the construction and maintenance of bone substance. This interrelation was clarified in a study using strain respectively flow which led to an activation of gadolinium-sensitive cation channels in ulnas in rats and calvarias in chicken. Integrins can be found in every cell of mammals (despite erythrocytes). They are receptors of the cell and crossing the cell membranes. Load-induced bone remodeling requires osteocytic integrins. This claim has been put in evidence due to studies concerning hind limb unloading of conditional knockout mice that were combined with a depletion of beta-1 integrins in the cortical bone and did not lead to a reduction of overall bone substance. In wild mice with non-depleted beta-1 integrins bone decomposition takes place. Therefore the Beta-1 integrin seems to be associated in the osteoclast formation (Rawlinson et al. 1996).

Primary cilia are known to be capable of sensing mechanical strain. They are also capable of anabolic signaling in osteoblasts and osteocytes. This ability was shown in a study in which osteogenic and bone resorptive responses to fluid flow required primary cilia. The primary cilia were deflected by fluid flow, triggering the anabolic signaling. This response was independent of  $\text{Ca}^{2+}$ -flux and stretch-activated ion channels (Malone et al. 2007).

---

### **3 Experimental design**

---

The following test design is performed over a series of twelve days to investigate the interdependencies of oxygen and glucose concentration on the osteogenic development capacities of adMSCs.

Cryo-preserved adMSCs of passage zero, derived from two different donors are revitalized and expanded in proliferation medium until the required cell amount is reached. Cells are strictly segregated into hypoxic (5% O<sub>2</sub>) and normoxic culture conditions. When confluence is reached, cells are seeded on 12-well plates in 2 mL proliferation medium. At a confluence stage of 80% the cell proliferation medium is exchanged for two different osteogenic media. One half is differentiated in customized DMEM (Dulbecco's Modified Eagle Medium) with additives of the synthetic glucocorticoid dexamethasone, L-ascorbic acid and beta glycerophosphate while the other half is differentiated in  $\alpha$ MEM (Minimum Essential Medium  $\alpha$ ) with a lower glucose concentration and the same amount and composition of additives. Measurements of glucose and lactate are performed on a daily basis for a better understanding of the cell development and adaption to different lactate conditions and glucose levels. To eliminate measurement implicit errors as far as possible an error curve is applied on the obtained values of glucose and lactate. Light microscopy is performed for every well in a four-day cycle, followed by morphological studies based on the gained pictures. One third of the plates undergo an examination in the beginning, one third in the middle and the last third in the end of the twelve-day investigation period to examine the progress in mineralization. After the plates are extracted and ethanol fixated, DAPI- and calcein-fluorescence microscopy assays are performed as well as alizarin red and von Kossa staining to monitor the ossification status in comparison to the amount of living cells.

---

## **4 Results and discussion**

---

The following chapter will contain analytical observations and assumptions based on findings derived of the four different staining sequences and their light microscopic analysis. In addition, the daily values of glucose and lactate will be taken into consideration.

### **4.1 Staining analysis**

The progression in the ossification development is monitored by the use of alizarin red and von Kossa staining. These two methods are widely used to detect the mineralization of the developing extracellular matrix. As bone consists of calcium phosphate, alizarin red displays the occurrence of calcium ions while von Kossa staining is a phosphate detection method.

Plates from differentiation day 0, 7 and 12 are withdrawn, fixated and stained. Each staining has at least one replicate. As von Kossa as well as alizarin red staining classify the ossification status, one can claim four replicates to be present for every combination of oxygen concentration with medium and donor.

To visualize the outcome in a plain manner for every well cultivated under the same conditions one well of average appearance is chosen to represent the staining result. Figure 6 is an ordered composition of these representative wells. Figure 7 contains every von Kossa and alizarin stained well including the staining references.

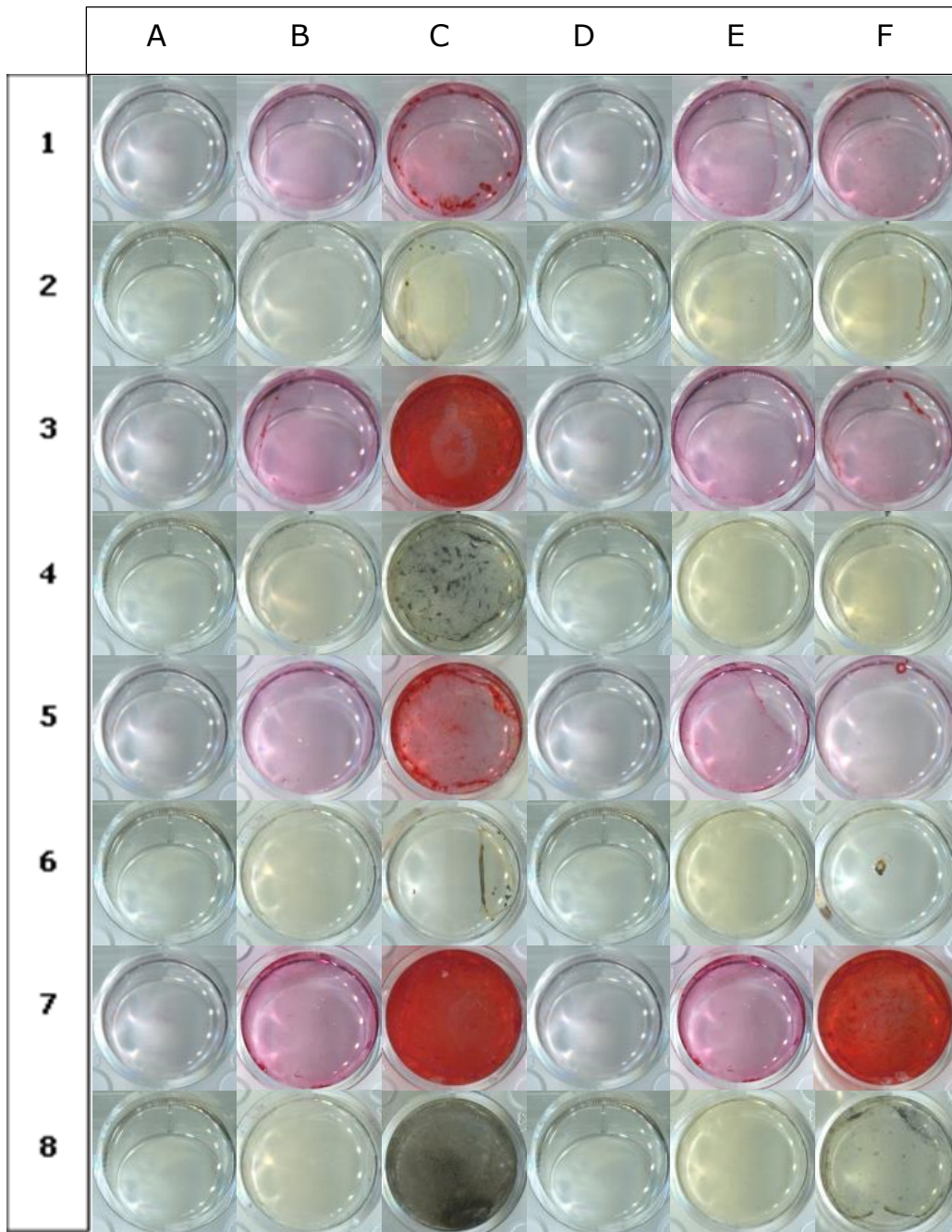


**Figure 6: Representative wells after staining; normoxia: A-C; hypoxia: D-F; qMEM: 1-4; DMEM: 5-8; donor A: 1-2 & 5-6; donor B: 3-4 & 7-8; alizarin red: odd-numbered; von Kossa: even-numbered; day 0: A&D; day 7: B&E; day 12: C&F**

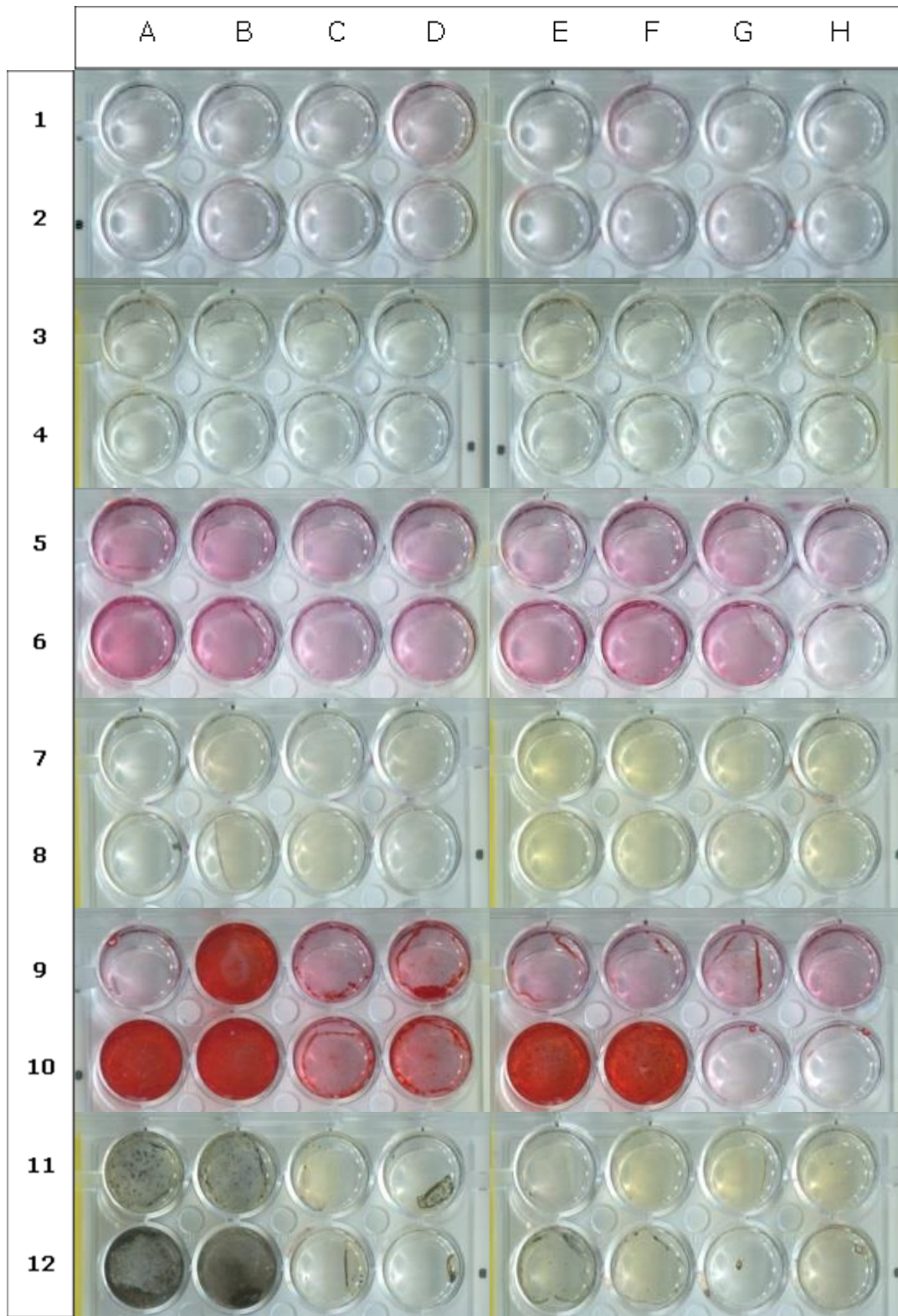


**Figure 7: Cultivation plates after staining; alizarin red: 1, 2, 5, 6, 9, 10; von Kossa: 3, 4, 7, 8, 11, 12; day 0: 1-4; day 7: 5-8; day 12: 9-12;  $\alpha$ MEM: odd-numbered; DMEM: even-numbered; donor A: A, B, E, F; donor B: C, D, G, H; normoxia: A-D; hypoxia: E-H**

Before the cell differentiation is induced a third of the initial plate amount is withdrawn and the inhabiting cells are stained in order to serve as a reference source to distinguish between real differences in the differentiation stage and the cells implicit staining capacity independent of the differentiation. The result shows a strongly mild violette color that can be distinguished easily from the staining capacity of samples from day 7 or day 12, respectively. Therefore, one can estimate the stage of differentiation in further stainings of alizarin just by the visual appearing of these dyed cell layers.

The different reference wells of day 0 hardly vary in their appearance. In general there is no major distinction between different oxygen concentrations, different media or stem cell donors. One well shows a slightly stronger staining. Since the replicate of the well does not show a similar observation, one can assume that this is caused by a slightly thicker cell layer due to different proliferation velocities after thawing and cryo-preservation. Especially for hypoxic cryo-preserved adMSCs from donor A lower proliferation velocity is observable as well as a lower alive-to-dead ratio after thawing. Other wells that exhibit the same culture conditions don't show the described behavior. As additionally hypoxic conditions were proven to promote proliferations by various research groups (D'Ippolito et al. 2006; Grayson et al. 2007), one has to assume that this observation is not caused by the cultivation itself but by the cryo-preservation process of the described cells.

At differentiation day 7 alizarin red stainings show severe differences in their staining intensity compared to the reference attesting an early stage calcium accumulation. The cell layers partially begin to lose their attachment to the plate. Their wrapped edges show a distinct higher intensity of color (see B3 and E5 in Figure 6) that could either be caused due to thicker tissue layers over the course of the wrapping processes or due to higher ossification rates caused by the threedimensional

framework. The more three-dimensional-like framework is assumed to better mimic physiological conditions. As cells of overlapping layers have an increased sphere of influence, secreted compounds with an ossification inducing effect are more likely to interfere with a wider area. It has been testified that contact of cells to ECM that did not originate from these certain cells can promote ossification development (Coan, Heather Adeline Bradbury 2011).

The following section concentrates on differences in cell layer staining intensity. The dye-ability analysis shows similar tendencies for differentiation day 7 and 12. Therefore for the sake of simplicity the further analysis refers to both day 7 and day 12. A more distinguished insight can be gained with the aid of diagrams presented in Figure 8. This diagram illustrates and clarifies the influences of different oxygen concentrations, media and cell donors on the staining intensity of cell layers withdrawn on day 7 and 12 during cultivation under equal conditions. It is based on an examination of stained wells. The fluorescence microscopes' adaption to the intensity of light is causing a less objective character of its results. Therefore, light microscopic shots are preferred for the classification of the chronological ossification development. The coping effect is chosen to get a better insight in the single stages of development; otherwise early stages cannot to be recognized due to lower light emission rates. Because highly ossified cell layers tend to detach, the differences are suggested to be even more significant for day 12 wells.

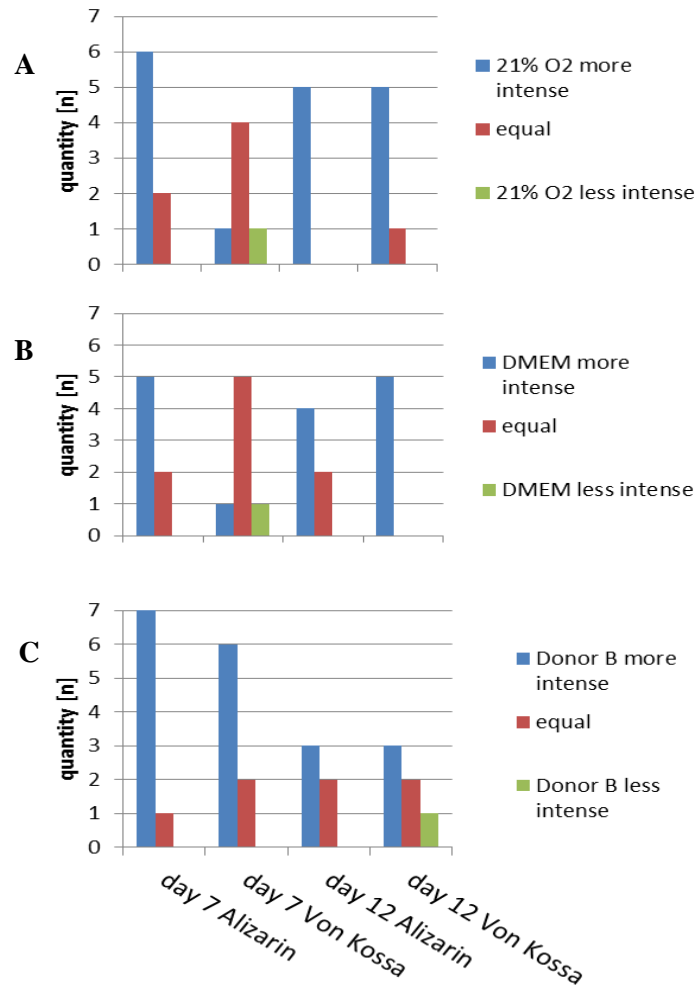


**Figure 8: Quantity of staining intensities of cell layers on differentiation day 7 and 12 dependent on oxygen concentration (A), culture media (B) and cell donor (C)**

### **Von Kossa staining analysis**

Similar to alizarin red stained wells von Kossa stained wells of differentiation day 0 are used as a reference source to distinguish between an inherent dyeing capacity and the dyeing that is only effected by the cell ossification status. As the cell layers of differentiation day 0 barely show any greyish staining effects, the classification of the mineralization status based on the plain visual staining is legit.

## **(A) Atmosphere**

Normoxic in comparison to hypoxic cultivation reveals the biggest differences in the varying differentiation conditions. Under normoxic conditions 11 out of 16 wells show stronger dyeing intensities, 2 cell layers show a similar intensity and in 3 out of 16 cases no assertion can be put up due to cell layer detachment.

The predominance of normoxia gets visible for the day-12 withdrawn cell culture dishes. For day-7 withdrawn dishes no distinction can be made, neither for alizarin-based nor for von Kossa-based staining. This brings up two suggestions. Either atmospheric influences are negligible in early phases compared to the ossification potential implemented by the additives, or that the provided oxygen is sufficient enough for the hypoxic conditions during the early phase but with increased cell layer thickness and thickened ECM, diffusion of oxygen is hindered, leading to insufficient levels of oxygen.

As analyzed in the chapter "Theoretical background" of the work on hand, the expected advantages of hypoxia differentiation by preserving the multipotent character of MSCs are not supposed to have an effect in short-time cultivation. The case above with an investigation period of 12 days and the use of passage 0 adMSC represents such a short-time cultivation. As discussed earlier D'Ippolito *et al.* proclaim hypoxia to be in general disadvantaged during differentiation. Two counter-arguments make the application of their hypothesis questionable. Firstly, the work of D'Ippolito *et al.* was performed with bone marrow derived MSCs rather than adMSCs and secondly, the study also included cells of passage 1, that don't comprise the long-term beneficial effect.

## **(B) Medium**

DMEM seems to have a stronger potential in terms of differentiating adMSCs towards the osteogenic lineage. DMEM affects either in a stronger staining in 9 out of 16 cases or it shows at least the same stain intensity in 4 cases. In 3 cases it is not possible to claim a specific influence due to cell layer detachment. In one case exclusively  $\alpha$ MEM produces a stronger staining compared to DMEM. According to a comparison between day-7 and day-12 withdrawn cell layers the tendency of DMEM to favor an early ossification rises over time during the 12-day sequence.

Similar to the corresponding section of alizarin red stained cell layers von Kossa staining analysis is done for differentiation day 7 and day 12 combined. In contrast to alizarin red stained wells von Kossa stained wells show less intensive staining differences between  $\alpha$ MEM and DMEM for day 7. Here 5 out of 8 wells have the same staining intensity, in one case  $\alpha$ MEM shows a higher dyeing intensity, in another case it is contrary and in one case a distinction cannot be done due to cell layer detachment. For day 12 a different behavior is observable. Here 5/8 wells are clearly stronger dyed when cultivated in DMEM compared to wells cultivated in  $\alpha$ MEM. Three out of 8 wells are indeterminable due to cell layer detachment. Compared to the examined alizarin-stained cells from differentiation day 7, the von Kossa stained cells show less dyeing intensity. For this case the dyeability is almost equally distributed.

## **(C) Donor**

For alizarin red and von Kossa staining the comparison of the wells, inhabiting donor-B adMSCs with wells inhabiting donor-A adMSCs proves donor-B stem cells to be superior in terms of the ossification velocity.

For alizarin red a single case of donor A cells results in a more intense staining compared to donor B cells. While 10 out of 16 exhibit a clearly

stronger staining when donor B cell layers are compared to donor A layers. Three wells possess the same intensity and for another 3 wells no claim can be made due to cell layer detachments. It is supposed that evidence for a higher or at least faster ossification potential of donor B adMSCs would be even stronger in the case of no detachment processes. These detachment processes are assumed to result in the seen downward oriented sequence in Figure 8, section C.

Von Kossa wells in combination with donor B cells exhibit a stronger coloring in 9 out of 16 times and the same staining intensity in 2 out of 16 times. For two wells no statement can be made due to cell layer detachment. In one well out of 16 the well inhabiting donor B adMSCs shows a less strong coloring compared to donor A adMSCs.

## **4.2 Microscopical analysis**

### **4.2.1 DAPI and calcein fluorescence analysis**

Figure 9 represents and highlights the average findings of fluorescence microscopy after incubation with DAPI and calcein solution. It is assembled in the same manner as in Figure 6 and Figure 10 and contains a high degree of similarity concerning their ossification status apart from E7 of Figure 9 that monitors different results for scans.

Areas where calcein highly accumulated show a lack of DAPI stained cells. Additionally cell-cell distances increase in average over time. DAPI intensity reaches its peak on day 7 and decreases from day 7 to day 12 resulting in a less equal distribution of living cells, indicating that mineral accumulation results in spatial scarcity and less viable conditions perhaps due to decreased nutrient and oxygen diffusion. This statement is endorsed by pictures of roundly wrapped cell layers without or with rare DAPI stained cells in the center as can be seen in sub-picture F5 of Figure 9 or in sub-picuture F1, F5 and B7 of Figure 11. In general, one can state

a high conformance comparing cellular development under equal oxygen conditions and cultivation in the same medium, meaning that one expects donor A cells to gain similar results compared with donor B cells when cultivated in the same medium and atmosphere (see F2 and F4 as well as B6 and B8). Normoxia does not only seem to accelerate the ossification development in this work but also seems to have advantages in terms of proliferation rates as Figure 9 seems to endorse. Here the lower confluence does not implicate a lower ossification rate as the sequence A1 to C2 reveals, where cells are less dense packed in comparison to other sequences but do exhibit calcein staining as early as after differentiation day 7. While focusing on the differences of normoxic to hypoxic cultivated cells, one recognizes hypoxia to not result in calcein accumulation after 7 days. In average only in 2 out of 12 cases (F6 and F8 of Figure 9) detectable amounts of calcein adsorption is monitored. Normoxia affects in an adsorption of calcein at the 7<sup>th</sup> day in 3 out of 4 cases on average. Considering studies of (Müller et al. 2008) where first ossifications are detected at differentiation day 8 and first slight positive tests for mineral accumulation of the work on hand are conducted at day 7, the author assumes that mineralization is not detectable earlier as on differentiation day 7.

In general cell layers cultured in DMEM medium gain higher staining intensities than in  $\alpha$ MEM. Donor A cells possess a higher ossification rate than donor B cells. The combination of DMEM medium and donor B cells tends to effect in homogenously distributed cells and comparable homogenously distributed ECM, inhabiting highly concentrated calcium depositions, on the well bottom (C8 in Figure 11 and Figure 6). These ECM depositions on the bottom of the cultivation dishes occur as early as on differentiation day 3 according to a study by Coan *et al.* (Coan, Heather Adeline Bradbury 2011). Sub-pictures B2, B6 and B8 of Figure 9 reveal an

insular development of early calcium accumulation considering that differentiation does not evenly spread across cell layers.

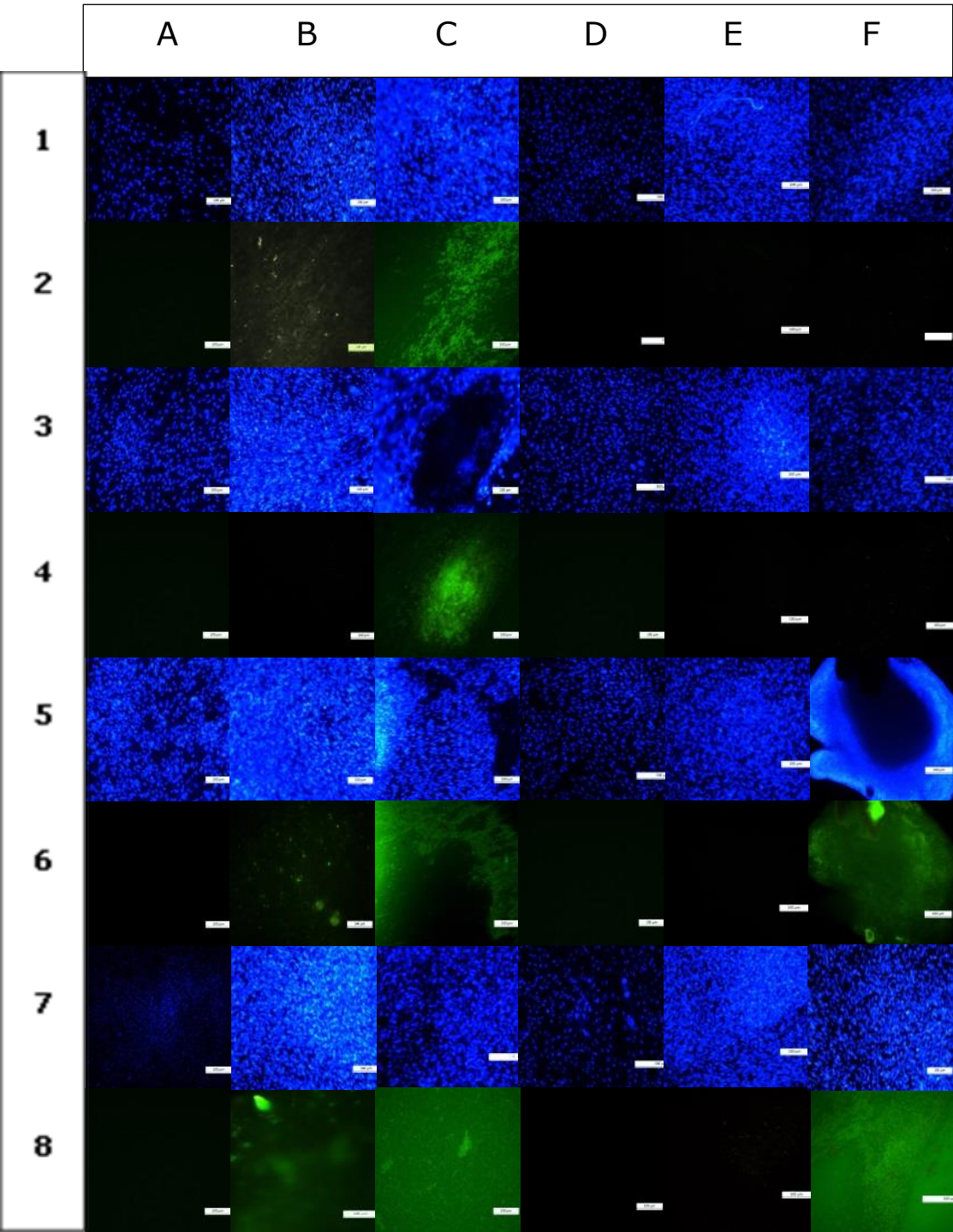
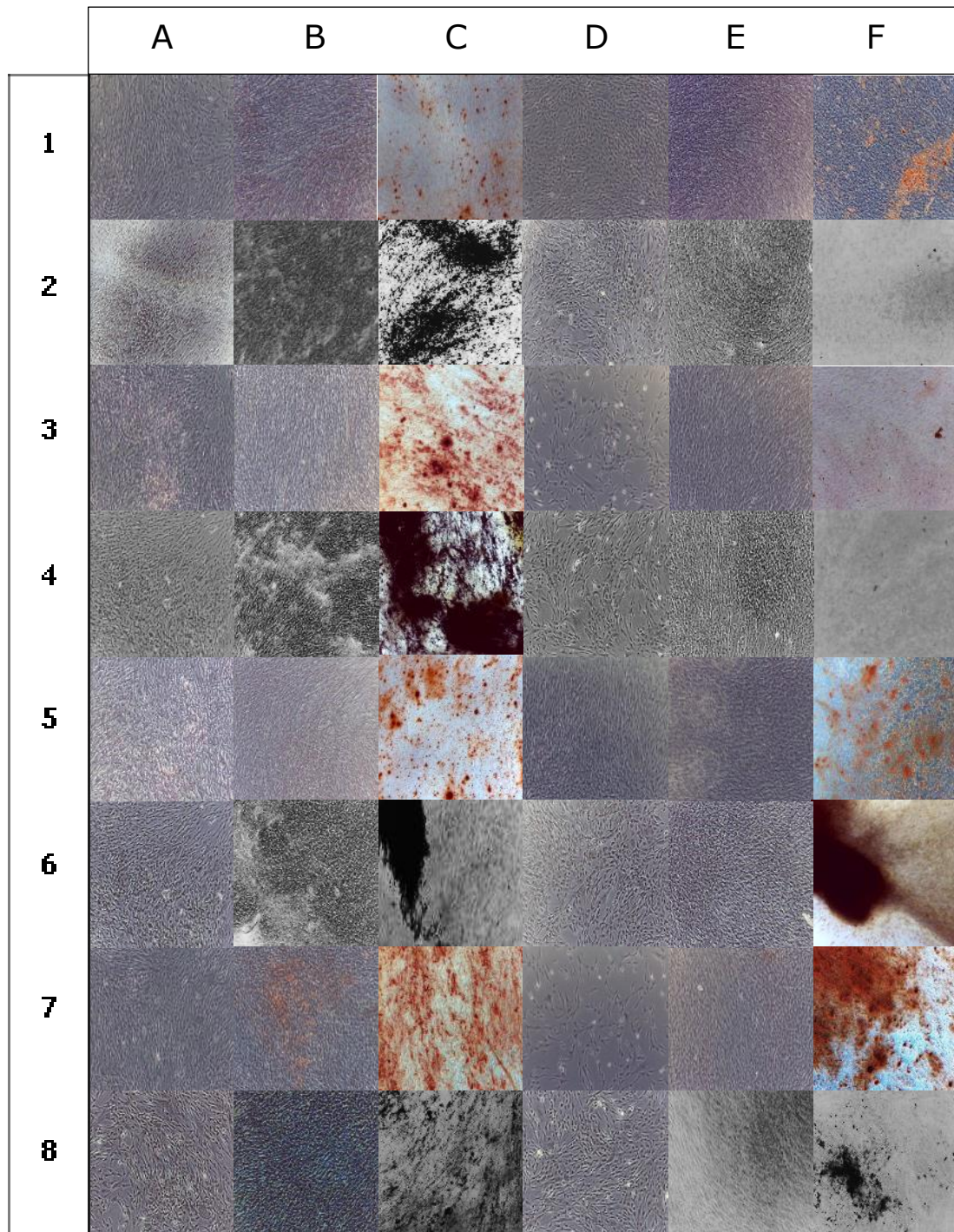


**Figure 9: Fluorescence microscopy after incubation with DAPI and calcein solution. normoxia: A-C; hypoxia: D-F;  $\alpha$ MEM: 1-4; DMEM: 5-8; donor A: 1-2 & 5-6; donor B: 3-4 & 7-8; DAPI: odd-numbered; calcein: even-numbered; day 0: A&D; day 7: B&E; day 12: C&F; length of scale bars equals 100  $\mu$ m**

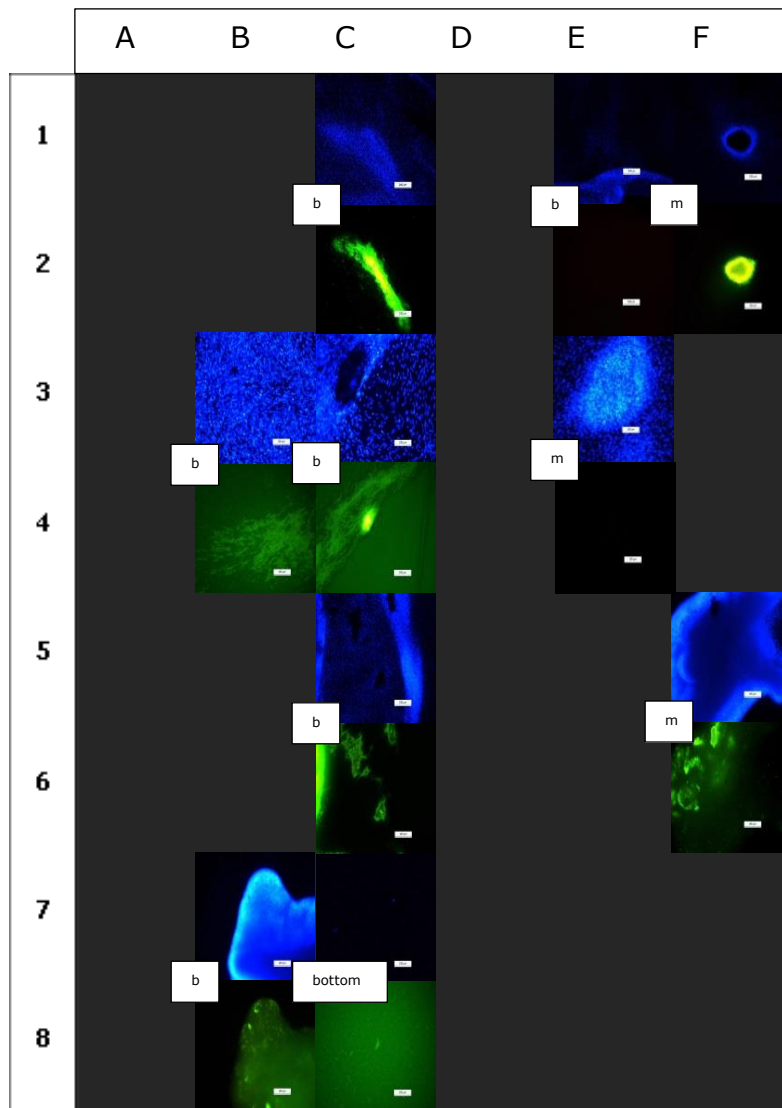
#### **4.2.2 Light microscopy and morphological analysis**

Figure 10 presents the ossification status of the single wells similar to former figures. Ossification velocities do not seem to match with fluorescence microscopy analysis. This observation is assumed to be caused by the adjustment of the used fluorescence microscope to the current light intensities as formerly described. For fluorescence microscopy with DAPI and calcein higher light intensity is proportional to a more intense staining. As the lens adjusts itself to lower light intensities, mineralization is monitored in an earlier stage compared to light microscopic methods.

Normoxic and DMEM cultivation have advantages in terms of ossification velocity. When hypoxia and normoxia are compared concerning their colony forming potential normoxia exhibits more colonies at differentiation day 12 testifying the findings of Basciano *et al.* for MSC passages zero to one (Basciano et al. 2011). The staining appearance of DMEM and donor B cell combinations is less heterogeneously distributed. This also applies for microscopic shots of unstained cell layers after fixation of Figure 13. Normoxia clearly shows more ossification in light microscopic and fluorescence microscopic pictures. Unlike Figure 9 and Figure 11 calcium accumulation does not seem to occur prior to phosphate accumulation. This may be due to differences in the minimum threshold of the tests. MSCs experiencing scarce sugar supply ( $\alpha$ MEM + hypoxia) exhibit a suppressed ossification development.



**Figure 10: Light microscopy after alizarin red and von Kossa staining. normoxia: A-C; hypoxia: D-F; gMEM: 1-4; DMEM: 5-8; donor A: 1-2 & 5-6; donor B: 3-4 & 7-8; alizarin red: odd-numbered; von Kossa: even-numbered; day 0: A&D; day 7: B&E; day 12: C&F**



**Figure 11: Fluorescence microscopy after incubation in DAPI and calcein solution – different from the norm. normoxia: A-C; hypoxia: D-F; qMEM: 1-4; DMEM: 5-8; donor A: 1-2 & 5-6; donor B: 3-4 & 7-8; DAPI: odd-numbered; calcein: even-numbered; day 0: A&D; day 7: B&E; day 12: C&F; b: near to the border of the well; m: middle of the well; b: border-near area; bottom: layer-detached well bottom area; length of scale bars equals 100  $\mu$ m**

Figure 11 shows, in contrast to Figure 9, shots of cell layers differing from default. As more abnormal findings are increasingly found near the well border, shots of stained cultures exhibit a legend on the side of each picture showing their local origin. Shots of the average cell layers are taken from areas near the center of the cell layer. This section deals with average aberration. Shots and findings differing from default that are not

mentioned here will be focused on in following sections more precisely. In total it is observable that hypoxia and DMEM cultivation result in more extreme findings, cell agglomerations and areas of very uneven spread and concentrated ossification. The closer cell layers grew to the borderline of the well, the more likely anomalous cell layer appearance gets. Wells that do not show ECM mineralization in Figure 6 and Figure 7 can possible exhibit areas of progressed ossification as can be seen in sub-pictures B4 and B8. The sub-section B4 of the staining analysis figures normally do not exhibit any staining. But in this abnormal case, calcein staining occurred in a small area on a plain well layer. For sub-picture B8 the cell layer wraps itself around, increasing the staining possibility due to vertically stacked staining particles.

As E1 and E3 of Figure 11 show a dense agglomeration of vivid cells without any calcium detection, the later ossification of cells under hypoxic conditions is not caused by lower proliferation velocities.

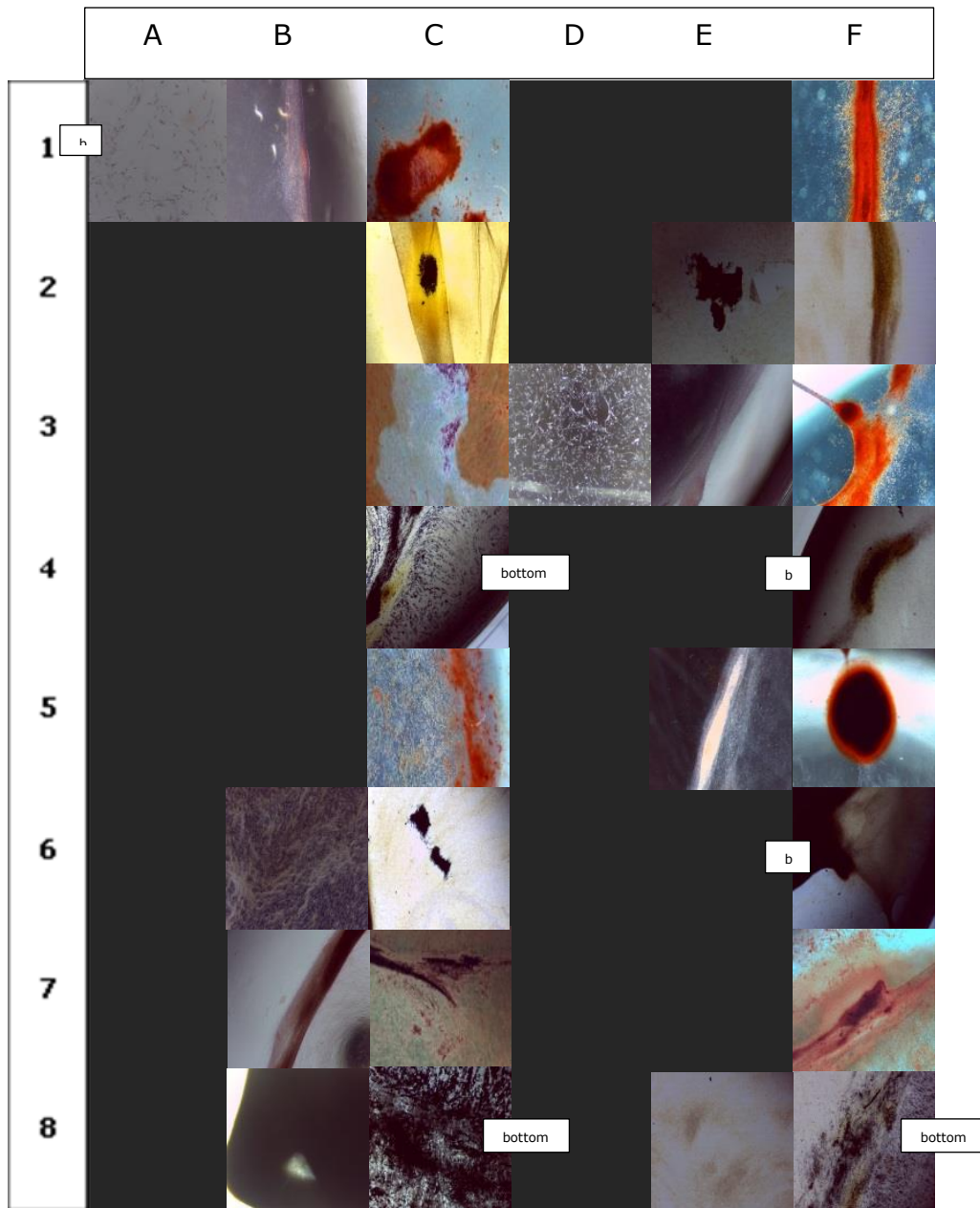


**Figure 12: Light microscopic pictures after alizarin red and von Kossa staining – different from the norm: normoxia: A-C; hypoxia: D-F; αMEM: 1-4; DMEM: 5-8; donor A: 1-2 & 5-6; donor B: 3-4 & 7-8; alizarin red: odd-numbered; von Kossa: even-numbered; day 0: A&D; day 7: B&E; day 12: C&F; b: border-near area; bottom: layer-detached well bottom area**

Sub-figures A1 and D3 of Figure 12 picture the borderline of cell layers at differentiation day zero. Confluence in areas near the well border on average is reached on differentiation day 7. Sub-figures C1, C2, C6 and E2 show a dense insular appearance of bony matrix maturation that can only be seen in this particular area in the middle of the well. More homogenously spread but with much smaller agglomerations, mineral

deposition is also recognized in areas near the borderline. Areas near the borderline show stronger ossification intensity. Considering the lower confluence of border-near areas at the beginning of this work, this finding is particularly noteworthy.

B6 shows similar insular mineral deposition in the well center but smaller clusters. The deposition is highly homogenously spread. F1, F2, F3, F4, F6, F7, E5, C5, B2 and B7 show borderlines of cell layers that are wrapped from the well borders towards the center of the well. These wrapped borderlines show a distinct stronger ossification compared to the average. That could either be caused due to more mechanical and pressure stimuli during medium exchange or due to the resulting three-dimensional structure that mimics physiological conditions more precisely. Combinations of these two are possible as well. On the bottom of wells C4, C8 and F8 of Figure 12 mineral accumulation can be seen without any cell layers covering this accumulation. Cells under C3 conditions develop a thick layer of red mucus like secretion that, if removed by the use of pipettes reveals insular, purple structures underneath. This mucus is assumed to be the preliminary ECM that according to studies of Xu *et al.* (2009) and Coan *et al* (2011) has positive feedback influences on the differentiation of surrounding MSCs.

B8 shows a roundly and totally wrapped cell layer in the middle of the well. The occurrence of a totally wrapped cell layer in this early stage is an exceptional incident.

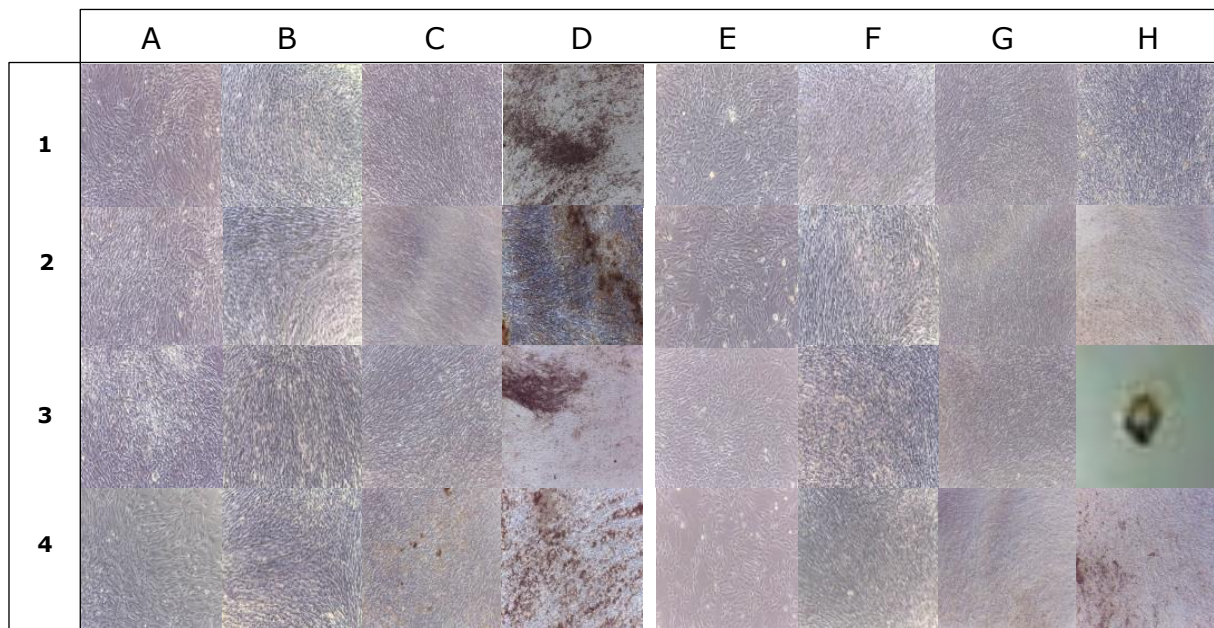


**Figure 13: Light microscopic pictures. normoxia: A-D; hypoxia: E-H; αMEM: 1-2; DMEM: 3-4; donor A: 1&3; donor B: 2&4; day 0: A&E; day 4: B&F; day 8: C&G; day 12: D&H**

The morphological analysis of Figure 13 shows the typical change in cell shape accompanied with a differentiation towards the osteogenic lineage (Jaiswal et al. 1997). While cells at differentiation day 0 show a spindle shaped fibroblast-like morphology, cells at day 4 or at least at the next microscopic examination day show a cuboidal shape. The thicker the cell layer gets and the more extracellular matrix is built up, the lesser the single cells are distinguishable. Mineral accumulation is not visible by eye before differentiation day 8. Similar to the light microscopic and fluorescence pictures of stained cell layers of Figure 9 and Figure 10 the first intense visible indicators of mineral precipitation are noticeable for donor B cells in DMEM under normoxic conditions. Here black dots appear in a selective manner in certain areas. For differentiation day 12 mineralization gets visible for every layer except for donor A cells in αMEM and hypoxia and donor B cells under the same conditions. For differentiation day 12 cell layers of donor B cells in hypoxia and DMEM are completely detached. But as sub-figure F6 of Figure 9 clearly reveals

intense DAPI and calcein fluorescent luminescence these cell layers have developed toward the osteogenic lineage. Shots of the different wells show similar stages of ossification independent from the method of detection. An exception from this claim is the combination of donor A cells with hypoxia and  $\alpha$ MEM that exhibits an alizarin red staining without being calcein stained or showing a mineral deposition in Figure 13. According to Figure 9, Figure 10 and Figure 13 where first mineral aggregation are noticeable at differentiation day 7 or 8, respectively, early ossification clearly benefits from normoxic culture conditions. Also cultivation in DMEM seems to be beneficial for an early ossification as Figure 9, Figure 10 and Figure 13 reveal strong mineral accumulation. The temporal appearance of the first ossification indications fits with the observations of Müller *et al.* (Müller *et al.* 2008).

As can be seen in D3 and D7 of Figure 10 as well as in E2 and E4 of Figure 13 cryo-preserved hypoxic cells of donor B seem to have a longer recovery phase from preservation conditions. During the first days after thawing the cultivated cells proliferate slowly, resulting in a slightly lower confluence stage of the several cell-medium-oxygen combinations. Nevertheless, these cells are able to regain the loss in time as donor B cells in DMEM and hypoxia reach one of the strongest staining results on day 12. Interestingly donor B cells in normoxia and DMEM, the combination with the earliest detection of matrix mineralization, has a strongly different appearance in the mineral deposition on differentiation day 12. Here, a dense, less scattered, diffuse mineralization coat builds up while other cell-medium-oxygen combinations lead to a punctual mineralization with a high amount of mineral free area.

According to DAPI staining of Figure 9 the cell count is increasing from differentiation day 0 to day 7 but decreasing from day 7 to day 12. This observation implies high proliferation rates in the beginning that strongly decline in the further course. The observation of high proliferation rates in

the beginning that decline in the further course is testified by the work of Coan *et al.* and Owen *et al* (Coan, Heather Adeline Bradbury 2011; Owen *et al.* 1990). A diagram representing their findings can be seen in Figure 14.

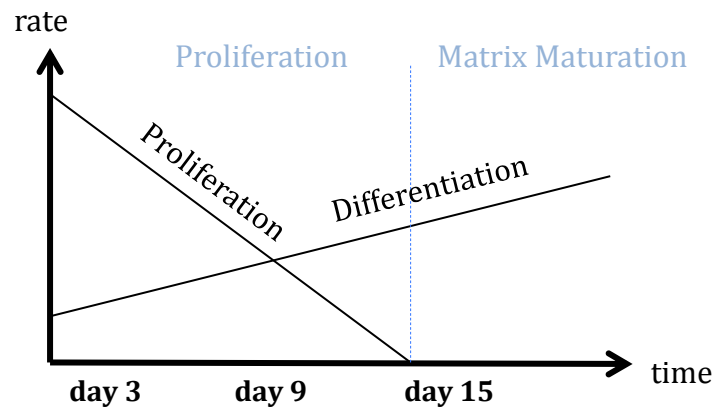


**Figure 14: Proliferation and ECM development during ossification**

As can be seen in C4 and C6 of Figure 9 highly mineralized areas don't host living cells. One explanation for this is the increasing volume of extracellular matrix. This claim is confirmed by the fact that cell-to-cell distances increase as well.

In the cases of cell layer detachments in late phases of the differentiation period a clearly visible mineral deposition is present (Figure 6, C8) on the wells' bottoms even if the cell layer is not present anymore.

### 4.2.3 Microscopic non-average findings

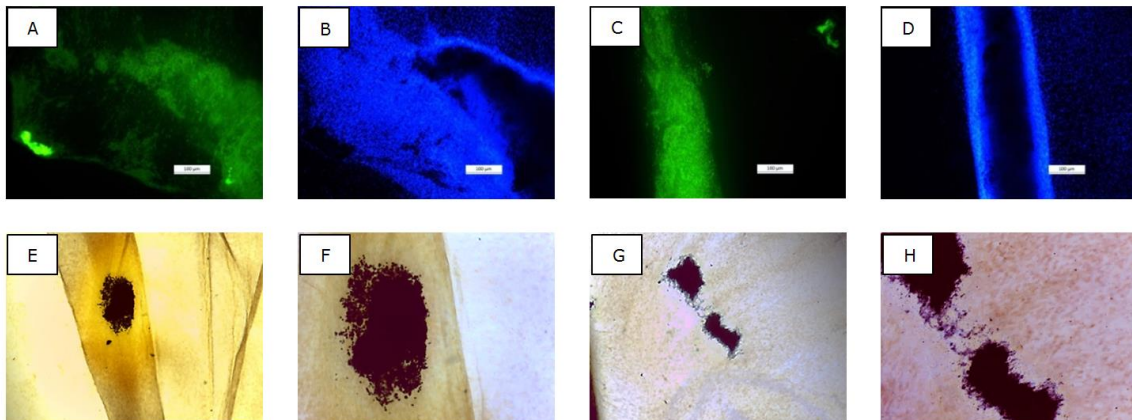


**Figure 15: Microscopical peculiarities of fluorescence and light-microscopic shots structured in a pairwise manner. A&B + C&D: calcein and DAPI staining; E&F + G&H: insular mineral deposition in two different amplification stages; length of scale bars: F & H, 100  $\mu$ m, others 500  $\mu$ m**

Figure 15 highlights some peculiarities and presents them in a bigger scale for a more detailed look. Shots of sub-figures A and B are taken from a wrapped cell layer of normoxic donor A cells on differentiation day 12 in  $\alpha$ MEM-differentiation medium. On the one hand they reveal highly mineralized areas to be free of living cells. On the other hand they are surrounded by a dense packed borderline of living cells. The thickness of this dense packed borderline does strongly vary. In this case the highly mineralized areas exhibit a rather wide area as well. The light microscopic shots marked C and D are cultivated under normoxic conditions. Their light microscopic pendant can be seen in F1 and F2 of Figure 12. Here a mineralized line, sometimes occurring even without cell layer detachment is enclosed by a thin area of dense packed living cells. Perhaps this line-formed characteristic has its origin in a differentiation signaling pathway that is transmitted in a unidirectional way. Pictures E to H are amplifications of formerly presented and discussed shots of Figure 12 showing the mineral deposition in a more precise way. Sub-figures E and F as well as G and H represent donor A cells under normoxic condition,

while E and F are nurtured by  $\alpha$ MEM- and G and H by DMEM-derived differentiation medium.

### **4.3 Glucose consumption, lactate production and LYR**

Measurements of glucose and lactate concentrations in the cell culture dishes are performed to gain insights in the metabolic adaptation and behavior concerning different oxygen and nutrient conditions.

Figure 16 shows the influence on the eight different single combinations of culture conditions on lactate production, glucose consumption and lactate yield ratio (LYR). Lactate yield ratio is an indicator for the proportion of lactic acid fermentation to aerobic respiration and therefore represents the metabolic efficiency. A higher LYR indicates lower metabolic efficiency. Another reason for the use of this parameter is its independence of cell counts. Due to this advantage the following analysis also focuses on varying values of the lactate yield coefficient. When general influences and tendencies of the differing media and atmospheres in the work on hand are clear, the scope of the following sections is transferred to time-dependencies of these influences. Unfortunately with the beginning of differentiation day 11 all cell layers of the special combination of donor A cells with hypoxic conditions are detached. To exclude these defective values the presented information in sub-figure F of Figure 16 concerning this special combination originates from values of the differentiation period from day 0 to day 10.

Donor B cells of hypoxia cultures possess the highest glucose consumption and lactate production rates, indicating strong growth and development processes, so one can assume these MSCs overcome the period of low reproduction rates after thawing resulting in lower-confluent cell layers on differentiation day zero.

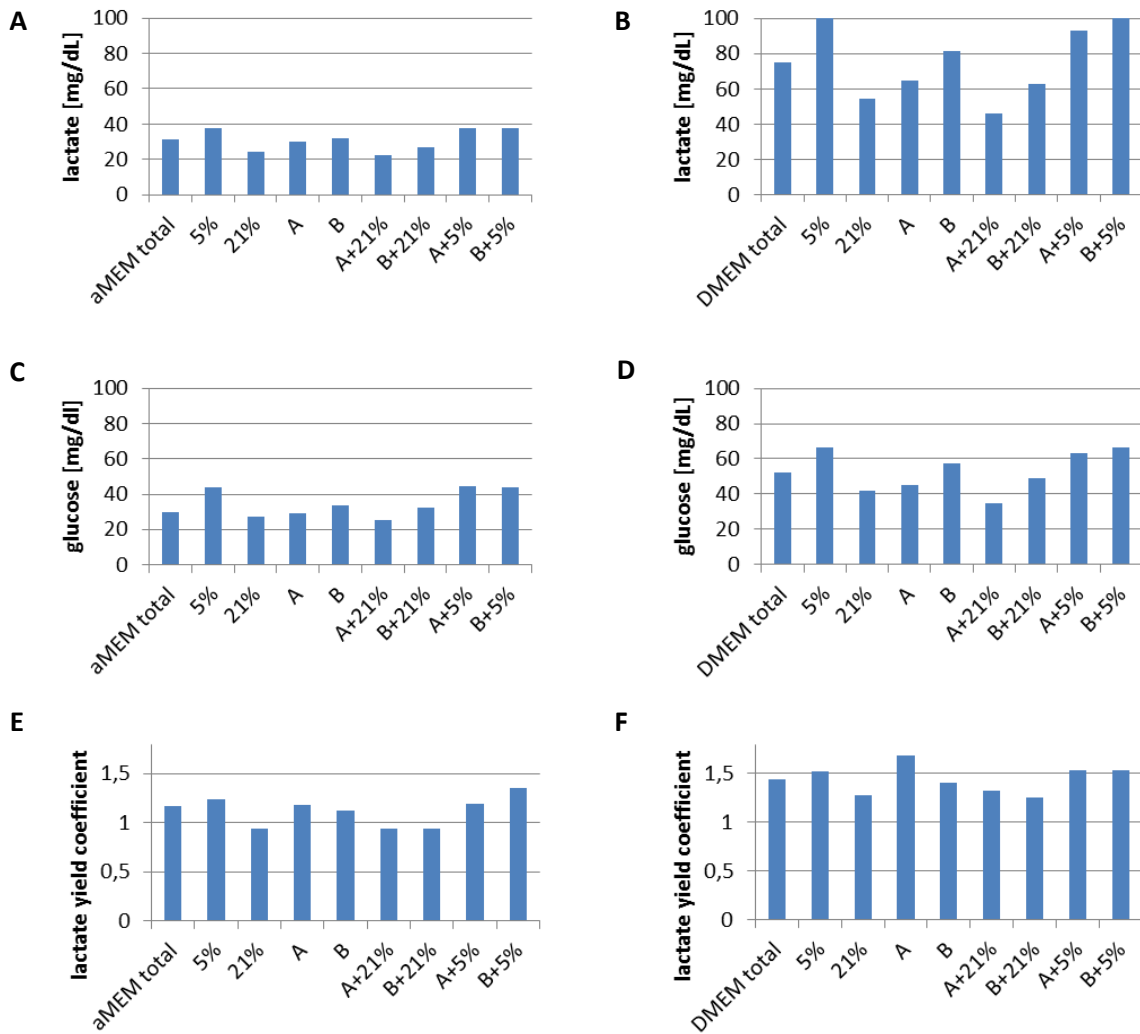


**Figure 16: Averaged daily values of lactate production, glucose consumption and lactate yield coefficient over the differentiation period of 12 days including their standard deviations for media aMEM and DMEM.**

Referring to the presented bar charts of Figure 16 hypoxia leads to higher LYR due to the lower partial pressure of oxygen. When hypoxia and normoxia are compared in terms of LYR, hypoxia exceeds normoxia by about 20-30% depending on the culture medium. This observation fits to Figure 16 and with a strong tendency to the time chart of Figure 22. These findings prove studies mentioned in the theory section that claim exceeding LYR values for hypoxia-cultured MSCs. These studies mention average LYR values for 2% oxygen cultivations of 2.5 and 1.7 for

normoxic cultivations. Values of the work on hand are lower and range from approximately 0.9 for  $\alpha$ MEM normoxia and 1.5 for DMEM hypoxia on average. Due to an assumed adaption period after switching from proliferation to differentiation medium, where LYRs are steadily near the just mentioned minimum value, averaged values would be higher if the adaption period is neglected. LYRs for the combination of DMEM with hypoxia conditions would average around the value 2. As lactate production is suppressed in a negative feedback with rising lactate concentrations due to the lactate dehydrogenase inhibition and lower sugar supply, the presented values are assumed to would have been higher with a steady nutrient supply and waste product exchange as it is done under chemostatic circumstances.

Lower oxygen concentrations tend to result in higher LYRs. As the work on hand performed all hypoxic cultivations with higher concentrations of oxygen than the cited study, it might be reasonably assumed that the mentioned values between 0.9 and 1.5 don't contradict the mentioned study. This applies even more when the adaption period and the effects of chemostatic conditions are also taken into consideration.

The use of DMEM as basic ingredient of the differentiation medium also leads to rising LYRs. Here LYRs exceed  $\alpha$ MEM-LYR values by approximately 30% on average. In the course of the higher energy supply this might be caused by the lower demand for cells to metabolically perform at the same efficiency as cells cultured with lower sugar concentrations like  $\alpha$ MEM-cultured cells. As  $\alpha$ MEM-based differentiation medium does not supply the cultured cells sufficiently, at least starting from differentiation day 12 for normoxia and from differentiation day 5 for hypoxia, DMEM-based values for lactate and glucose should represent the impact of atmosphere and nutrient feed more satisfactory.

Lower LYR values correlate with stronger ossifications on average. Although the usage of  $\alpha$ MEM-based medium leads to lower LYRs cells mineralize better under the use of DMEM-based medium. This observation is assumed to be caused due to the disadvantage of  $\alpha$ MEM-based media to supply the differentiating cells sufficiently. One reason for this correlative behavior between lower LYRs and higher mineralization might be the negative impact of high lactate concentrations on the differentiation process. As this argument gets invalidated in the further course other reasons have to be considered. In general and in comparison with Figure 5 higher glucose consumptions lead to more intense ossifications. Donor B cells metabolized approximately 30% more glucose. Bar charts for DMEM and  $\alpha$ MEM do correlate and match in a qualitative manner with a rather small exclusion for the combination B+5%. DMEM values for LYR normally exceed  $\alpha$ MEM values for about 30%.

Maximum overall LYR of the different combinations is around 1.6. If glucose would be considered as the only chemical source for lactate production, values exceeding 1.6 LYR are equivalent to a lactic-acid-fermentation to aerobic respiration ratio higher than 80%. Minimum ratios are around 63% for DMEM and 47% for  $\alpha$ MEM. As glucose is not the only energy source present in the cell culture medium that is metabolized into lactate the actual ratio is lower.

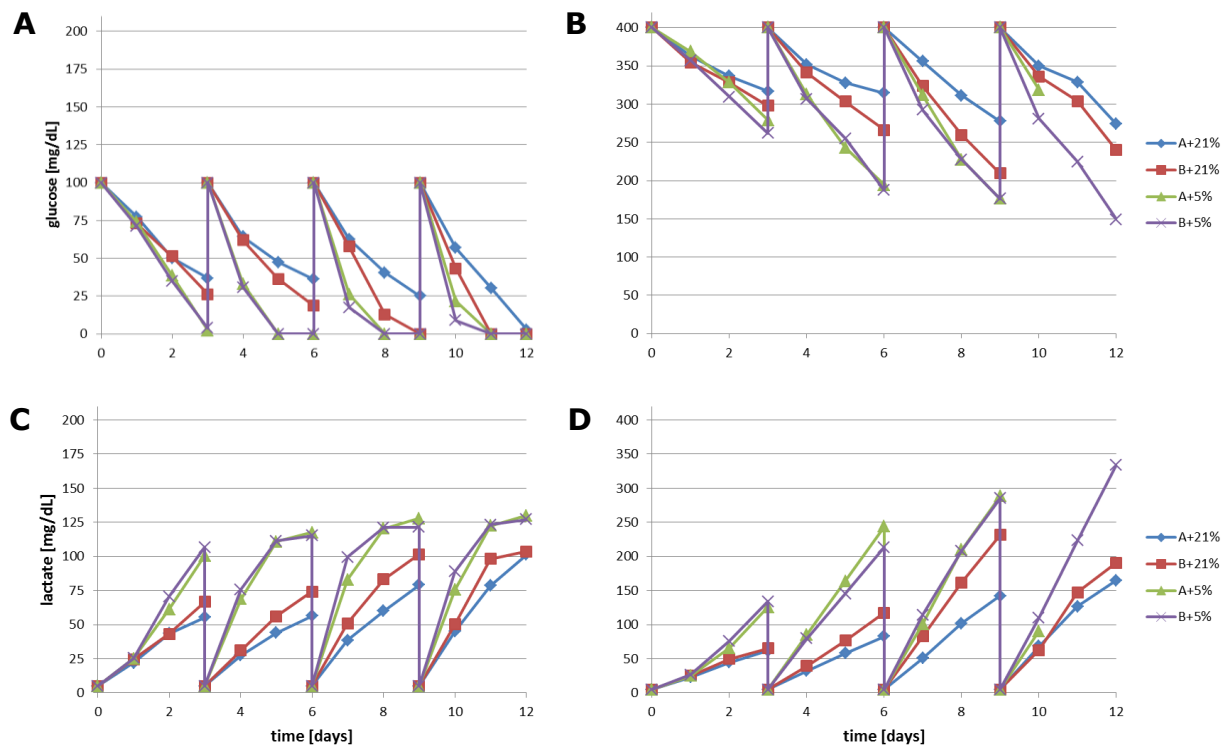


**Figure 17: Average glucose and lactate concentration over time; A: glucose levels in  $\alpha$ MEM-based medium; B: glucose concentration in DMEM-based medium; C: lactate accumulation in  $\alpha$ MEM-based medium; D: lactate accumulation in DMEM-based medium**

Figure 17 displays the strongly cyclic character in terms of average glucose and lactate concentrations. This is caused by the batch cultivation method where nutrient and waste products are not equilibrated in a small range but decrease in their concentration or accumulate, respectively until the volume is totally exchanged with new differentiation medium. This applies to the variant culture conditions. The diagrams as well as the already discussed Figure 16 state that some combinations result in an increased glucose consumption and lactate production compared to others. Donor B cells cultured in hypoxia consume the most glucose while a combination of donor A cells and normoxia result in minimum overall glucose consumption rates.

Due to the combinations of the various atmospheric and nutrient conditions it is necessary for a sufficient overview to present the single time-dependent charts and curves in one diagram. By doing so, different behavior in terms of time and corresponding relativities of the curves are more obvious. When standard deviations of these diagrams, concluding 4 different curves, are added, the diagram loses its clarity and clearness. Therefore one has chosen to specify variances of the several curves in a numbered way. To overcome the relation of standard deviations to increase with the absolute value, the coefficient of variation ( $c_v$ ) is also displayed, as can be seen in Figure 21. Here the coefficient of variation is represented by values beginning with zero. The use of the coefficient of variation guarantees the comparableness of variations in higher and lower curves as they for instance occur in lower aMEM and higher DMEM curve progressions.

$$c_v = \frac{\sigma}{\mu} \quad (1)$$

The coefficient of variation is defined as the ratio of standard deviation and the mean of the sample. It shows the extent of variability in relation to the mean of the population.

| A     | 1    | 2    | 3    | 4    | 5    | 6    | 7     | 8    | 9    | 10   | 11    | 12   |
|-------|------|------|------|------|------|------|-------|------|------|------|-------|------|
| A+21% | 3,29 | 2,03 | 3,86 | 1,71 | 4,11 | 6,13 | 4,40  | 6,47 | 4,71 | 2,18 | 2,78  | 5,93 |
|       | 0,18 | 0,06 | 0,08 | 0,07 | 0,09 | 0,09 | 0,11  | 0,08 | 0,04 | 0,04 | 0,03  | 0,05 |
| B+21% | 4,06 | 1,93 | 5,16 | 2,63 | 4,56 | 5,71 | 3,79  | 4,72 | 7,18 | 8,46 | 13,77 | 9,03 |
|       | 0,21 | 0,05 | 0,10 | 0,08 | 0,08 | 0,06 | 0,06  | 0,04 | 0,04 | 0,17 | 0,12  | 0,06 |
| A+5%  | 1,26 | 2,74 | 6,36 | 3,66 | 5,13 | 5,43 | 15,17 | 1,41 | 3,27 | 0,00 | -     | -    |
|       | 0,06 | 0,05 | 0,06 | 0,05 | 0,04 | 0,03 | 0,19  | 0,01 | 0,01 | 0,00 | -     | -    |
| B+5%  | 0,97 | 4,84 | 8,71 | 1,72 | 7,03 | 5,88 | 5,01  | 5,36 | 8,50 | 9,99 | 3,70  | 7,25 |
|       | 0,05 | 0,08 | 0,08 | 0,03 | 0,06 | 0,03 | 0,06  | 0,03 | 0,04 | 0,12 | 0,02  | 0,03 |

| B     | 1    | 2    | 3    | 4    | 5    | 6    | 7    | 8     | 9     | 10    | 11    | 12    |
|-------|------|------|------|------|------|------|------|-------|-------|-------|-------|-------|
| A+21% | 2,09 | 6,36 | 5,50 | 1,91 | 4,10 | 2,51 | 1,63 | 1,04  | 4,58  | 2,59  | 2,33  | 5,80  |
|       | 0,10 | 0,15 | 0,10 | 0,07 | 0,09 | 0,04 | 0,04 | 0,02  | 0,06  | 0,06  | 0,03  | 0,06  |
| B+21% | 4,67 | 3,84 | 6,09 | 3,22 | 5,15 | 5,11 | 5,57 | 10,14 | 11,11 | 11,82 | 18,52 | 10,00 |
|       | 0,19 | 0,09 | 0,11 | 0,10 | 0,09 | 0,07 | 0,11 | 0,12  | 0,11  | 0,24  | 0,19  | 0,10  |
| A+5%  | 3,92 | 4,72 | 7,50 | 2,12 | 4,91 | 2,79 | 8,19 | 2,97  | 2,81  | 8,76  | 1,60  | 1,65  |
|       | 0,16 | 0,08 | 0,07 | 0,03 | 0,04 | 0,02 | 0,10 | 0,02  | 0,02  | 0,12  | 0,01  | 0,01  |
| B+5%  | 3,67 | 4,72 | 7,38 | 2,27 | 4,62 | 2,16 | 2,14 | 2,12  | 2,49  | 17,10 | 3,02  | 2,58  |
|       | 0,14 | 0,07 | 0,07 | 0,03 | 0,04 | 0,02 | 0,02 | 0,02  | 0,02  | 0,19  | 0,02  | 0,02  |

**Figure 18: Standard deviations and coefficients of variations for lactate for DMEM (A) and  $\alpha$ MEM (B) regarding the absolute values**

| C     | 1     | 2     | 3     | 4     | 5     | 6     | 7     | 8     | 9     | 10    | 11    | 12    |
|-------|-------|-------|-------|-------|-------|-------|-------|-------|-------|-------|-------|-------|
| A+21% | 6,73  | 8,01  | 8,65  | 14,23 | 11,58 | 14,39 | 12,70 | 14,40 | 13,29 | 21,86 | 23,54 | 20,69 |
|       | 0,02  | 0,02  | 0,03  | 0,04  | 0,03  | 0,04  | 0,03  | 0,05  | 0,05  | 0,06  | 0,07  | 0,07  |
| B+21% | 12,98 | 10,46 | 8,01  | 11,28 | 5,45  | 14,59 | 11,12 | 15,22 | 9,34  | 7,04  | 20,87 | 9,94  |
|       | 0,04  | 0,03  | 0,03  | 0,03  | 0,02  | 0,05  | 0,03  | 0,06  | 0,04  | 0,02  | 0,07  | 0,04  |
| A+5%  | 16,07 | 14,97 | 10,17 | 9,30  | 6,93  | 11,26 | 22,97 | 10,34 | 8,81  | -     | -     | -     |
|       | 0,04  | 0,04  | 0,04  | 0,03  | 0,03  | 0,06  | 0,07  | 0,04  | 0,05  | -     | -     | -     |
| B+5%  | 9,12  | 11,24 | 11,22 | 6,78  | 3,95  | 6,85  | 7,92  | 14,77 | 9,60  | 5,36  | 5,07  | 8,96  |
|       | 0,02  | 0,04  | 0,04  | 0,02  | 0,02  | 0,03  | 0,03  | 0,06  | 0,05  | 0,02  | 0,02  | 0,06  |

| D     | 1    | 2    | 3     | 4    | 5    | 6    | 7    | 8    | 9    | 10   | 11   | 12   |
|-------|------|------|-------|------|------|------|------|------|------|------|------|------|
| A+21% | 8,02 | 4,90 | 14,25 | 3,76 | 6,21 | 5,96 | 3,59 | 6,07 | 2,82 | 6,45 | 2,17 | 4,76 |
|       | 0,10 | 0,10 | 0,39  | 0,06 | 0,13 | 0,16 | 0,06 | 0,15 | 0,11 | 0,11 | 0,07 | 1,73 |
| B+21% | 1,67 | 2,65 | 8,08  | 2,72 | 3,80 | 3,91 | 6,43 | 5,20 | -    | 3,03 | -    | -    |
|       | 0,02 | 0,05 | 0,31  | 0,04 | 0,10 | 0,21 | 0,11 | 0,40 | -    | 0,07 | -    | -    |
| A+5%  | 8,06 | 4,04 | 6,09  | 3,51 | -    | -    | 9,84 | -    | -    | 9,03 | -    | -    |
|       | 0,11 | 0,10 | 2,65  | 0,11 | -    | -    | 0,38 | -    | -    | 0,42 | -    | -    |
| B+5%  | 3,88 | 2,35 | 6,82  | 1,79 | -    | -    | 4,34 | -    | -    | 9,07 | -    | -    |
|       | 0,05 | 0,07 | 1,74  | 0,06 | -    | -    | 0,25 | -    | -    | 1,01 | -    | -    |

**Figure 19: Standard deviations and coefficients of variations for glucose for DMEM (A) and  $\alpha$ MEM (B) regarding the absolute values**

Section A in comparison to section B displays that cultivation in  $\alpha$ MEM-based medium partially results in glucose levels lower than detectable, noted as zero. The low values of glucose present in  $\alpha$ MEM-cultivated wells results in strongly cyclic glucose consumption and lactate production rates. Section A and B of Figure 22 confirm this claim. With the beginning of differentiation day 4 a clear cyclic behavior concerning the pictured values is observable. They are observable in the way that glucose consumption and lactate productions rates are high shortly after medium exchanges and low shortly before medium exchanges. The reason why this behavior does not apply for the period from differentiation day 0 to day 3 might be an adaption phase to the initiated differentiation processes beginning with the switch from proliferation to differentiation medium and the corresponding cellular stress. For the mentioned period beginning with differentiation day 4, the average glucose consumption rate for  $\alpha$ MEM-based cultivations per day decreases from about 80 mg/dL at days after medium exchange to about 10 mg/dL on the third day after medium exchange. This cyclic behavior does more precisely apply to  $\alpha$ MEM cultured cells but is still present for DMEM cultivations. For DMEM cultured MSCs the cyclic behavior concerning the lactic acid production is not significantly correlated with the amount of already present lactate concentrations in the medium, stating that concentrations of 125 mg/dL lactate are not suggested to impede lactate synthesis due to the lactate dehydrogenase inhibition.

As the color of the used differentiation media do not shift, indicating unacceptable pH values, pH values stay in the appropriate range over the course of the experiment. Therefore another possibly ossification suppressing reason can be eliminated.

| <b>A</b> | 1    | 2    | 3    | 4    | 5    | 6    | 7     | 8     | 9     | 10    | 11    | 12   |
|----------|------|------|------|------|------|------|-------|-------|-------|-------|-------|------|
| A+21%    | 4,18 | 4,95 | 3,05 | 2,17 | 3,66 | 2,80 | 5,59  | 1,89  | 5,45  | 2,77  | 1,71  | 4,24 |
|          | 0,18 | 0,23 | 0,18 | 0,07 | 0,14 | 0,11 | 0,11  | 0,04  | 0,14  | 0,04  | 0,03  | 0,11 |
| B+21%    | 5,16 | 4,25 | 4,99 | 3,34 | 4,09 | 4,50 | 4,81  | 5,93  | 9,23  | 10,75 | 24,28 | 6,29 |
|          | 0,21 | 0,17 | 0,32 | 0,08 | 0,11 | 0,11 | 0,06  | 0,08  | 0,13  | 0,17  | 0,29  | 0,15 |
| A+5%     | 1,60 | 3,25 | 7,88 | 4,66 | 4,24 | 4,81 | 37,93 | 44,60 | 34,19 | -     | -     | -    |
|          | 0,06 | 0,08 | 0,13 | 0,05 | 0,05 | 0,06 | 0,43  | 0,58  | 0,58  | -     | -     | -    |
| B+5%     | 1,23 | 6,02 | 9,27 | 2,19 | 7,92 | 4,92 | 6,36  | 1,41  | 9,90  | 12,69 | 10,79 | 9,00 |
|          | 0,05 | 0,12 | 0,16 | 0,03 | 0,12 | 0,07 | 0,06  | 0,01  | 0,13  | 0,12  | 0,10  | 0,08 |

| <b>B</b> | 1    | 2    | 3    | 4    | 5    | 6    | 7    | 8    | 9    | 10    | 11    | 12    |
|----------|------|------|------|------|------|------|------|------|------|-------|-------|-------|
| A+21%    | 2,09 | 5,27 | 7,68 | 1,91 | 3,22 | 3,20 | 1,63 | 2,81 | 4,74 | 2,59  | 2,03  | 3,65  |
|          | 0,10 | 0,25 | 0,64 | 0,07 | 0,19 | 0,26 | 0,04 | 0,13 | 0,25 | 0,06  | 0,06  | 0,16  |
| B+21%    | 4,67 | 4,52 | 6,57 | 3,22 | 4,21 | 1,75 | 5,57 | 4,66 | 3,25 | 11,82 | 8,94  | 12,33 |
|          | 0,19 | 0,24 | 0,53 | 0,10 | 0,17 | 0,10 | 0,11 | 0,15 | 0,18 | 0,24  | 0,19  | 2,21  |
| A+5%     | 3,92 | 6,05 | 7,73 | 2,12 | 3,87 | 4,49 | 8,19 | 5,76 | 1,79 | -     | -     | -     |
|          | 0,16 | 0,17 | 0,20 | 0,03 | 0,09 | 0,67 | 0,10 | 0,15 | 0,24 | -     | -     | -     |
| B+5%     | 3,67 | 5,05 | 7,59 | 2,27 | 4,20 | 2,81 | 2,14 | 1,33 | 2,35 | 17,10 | 17,64 | 3,86  |
|          | 0,14 | 0,11 | 0,21 | 0,03 | 0,12 | 0,73 | 0,02 | 0,06 | 4,93 | 0,19  | 0,51  | 1,02  |

**Figure 20: Standard deviations and coefficients of variations for lactate for DMEM (A) and  $\alpha$ MEM (B) regarding the daily changes**

| <b>C</b> | 1    | 2     | 3     | 4     | 5     | 6     | 7     | 8     | 9     | 10    | 11    | 12    |
|----------|------|-------|-------|-------|-------|-------|-------|-------|-------|-------|-------|-------|
| A+21%    | 6,73 | 13,13 | 10,77 | 13,08 | 14,79 | 7,68  | 12,70 | 6,50  | 3,27  | 21,86 | 8,84  | 6,93  |
|          | 0,23 | 0,49  | 0,53  | 0,37  | 0,51  | 0,56  | 0,35  | 0,14  | 0,10  | 0,52  | 0,41  | 0,12  |
| B+21%    | 7,91 | 12,32 | 10,42 | 11,28 | 14,27 | 11,69 | 11,12 | 16,90 | 11,28 | 7,04  | 27,60 | 20,44 |
|          | 0,25 | 0,38  | 0,34  | 0,22  | 0,37  | 0,31  | 0,16  | 0,28  | 0,22  | 0,13  | 0,84  | 0,31  |
| A+5%     | 6,98 | 14,58 | 11,30 | 9,30  | 11,35 | 7,07  | 23,38 | 23,33 | 11,84 | 13,77 | 7,29  | 11,45 |
|          | 0,25 | 0,41  | 0,22  | 0,12  | 0,16  | 0,14  | 0,30  | 0,37  | 0,26  | 0,25  | 0,39  | 0,23  |
| B+5%     | 9,12 | 14,93 | 17,25 | 6,78  | 7,96  | 5,86  | 7,92  | 13,52 | 12,87 | 5,36  | 7,83  | 6,22  |
|          | 0,27 | 0,30  | 0,36  | 0,08  | 0,15  | 0,14  | 0,08  | 0,19  | 0,25  | 0,05  | 0,14  | 0,08  |

| <b>D</b> | 1    | 2    | 3     | 4    | 5    | 6    | 7    | 8    | 9    | 10   | 11   | 12    |
|----------|------|------|-------|------|------|------|------|------|------|------|------|-------|
| A+21%    | 2,12 | 5,06 | 11,58 | 3,76 | 6,28 | 5,54 | 3,59 | 8,22 | 3,52 | 6,45 | 6,45 | 5,28  |
|          | 0,08 | 0,21 | 0,68  | 0,10 | 0,38 | 0,49 | 0,10 | 0,40 | 0,23 | 0,15 | 0,15 | 0,20  |
| B+21%    | 1,67 | 3,88 | 9,56  | 2,72 | 2,87 | 4,31 | 6,43 | 3,84 | 5,16 | 6,08 | 6,08 | 17,16 |
|          | 0,06 | 0,18 | 0,52  | 0,07 | 0,11 | 0,24 | 0,15 | 0,10 | 0,45 | 0,10 | 0,10 | 0,51  |
| A+5%     | 3,49 | 6,22 | 6,06  | 3,51 | 3,51 | -    | 9,84 | 6,65 | -    | 9,03 | 9,03 | 9,03  |
|          | 0,12 | 0,19 | 0,17  | 0,05 | 0,11 | -    | 0,13 | 0,23 | -    | 0,12 | 0,12 | 0,42  |
| B+5%     | 3,88 | 4,63 | 5,81  | 1,79 | 1,79 | -    | 4,34 | 4,39 | -    | 9,07 | 9,07 | 9,07  |
|          | 0,13 | 0,13 | 0,19  | 0,03 | 0,06 | -    | 0,05 | 0,23 | -    | 0,10 | 0,10 | 1,01  |

**Figure 21: Standard deviations and coefficients of variations for glucose for DMEM (A) and  $\alpha$ MEM (B) regarding the daily changes**

The maximum LYR of the  $\alpha$ MEM-based medium at differentiation day 11 must not strictly have a logical reason but can be the result of multiplying variances due to frictional arithmetic of two failure immanent parameters. These affects add up with glycolytic sources besides sugar like L-

glutamine contained in the differentiation medium that increase the overall lactate concentration.

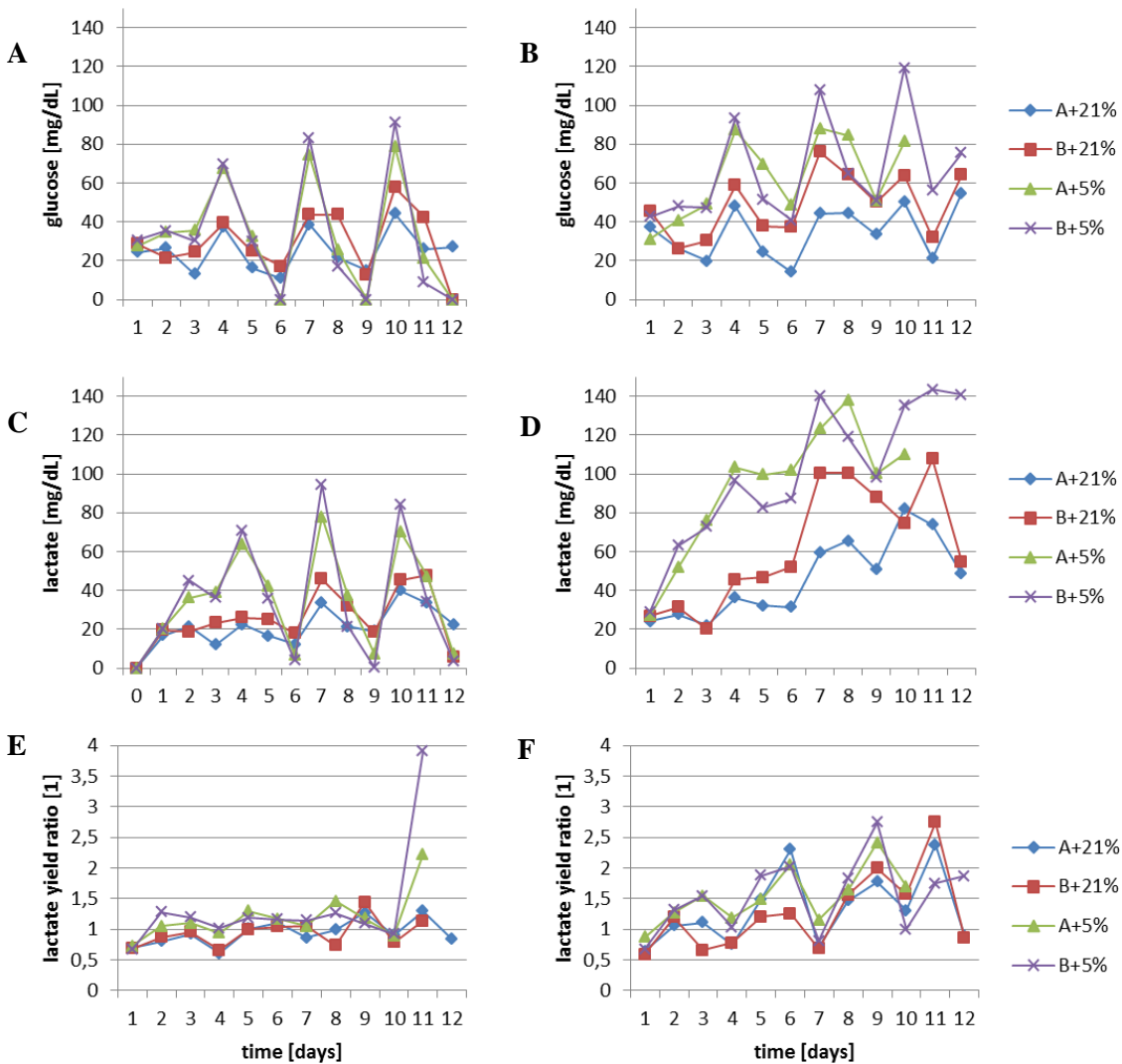


**Figure 22: Daily values for glucose, lactate and LYR; A-B: glucose consumption, C-D: lactate production, E-F: lactate yield ratio; αMEM time charts on the left, DMEM time charts on the right**

The rising LYR for DMEM over the course of the experiment might be partially explainable due to oxygen depleting effects within the cell layers accompanied with EMC maturation and cell layer thickening (Malladi et al. 2006). Additionally the increased oxygen consumption during osteogenic

differentiation of MSCs that implies rising LYRs might increase the LYR as well (Wang et al. 2005).

Interestingly glucose consumption possesses cyclic tendencies for DMEM nurtured cultures. As DMEM provides excessive amounts of glucose, scarce glucose supply can't explain this behavior. Therefore accumulating metabolites are highly suggested to decrease the glucose metabolism. When these metabolites are removed by the every-three-day medium changes, glucose consumption rises, but decreases until the next medium change.

Peculiar is the almost doubled lactate production rate under hypoxic conditions cultured in DMEM-differentiation medium. Hypoxic  $\alpha$ MEM-based cultures exhibit heightened lactate values as well but the differences get adjusted to one another due to the sugar supply deficiencies. There is the tendency for glucose consumption and lactate production to increase during the course of differentiation. In the beginning this tendency correlates with the proliferation rate and therefore the increase in the cell account. After the increased proliferation phase the rising glucose consumption is correlated with the need of the ECM to mature and mineralize.

#### **4.4 Mechanical promotion of osteogenesis**

Although the differentiation adMSCs and their maturing ECM does not comprise entrapped osteocytes, the osteoblast-like cells are able to function in the same osteogenic development promoting way. As the pipettes are not able to enforce high rates of whole tissue strains on the cell layers, they are not suggested to participate in the differentiation process. The same applies to hydrostatic pressure for the same reason. The remaining possibilities causing the increased mineralization of

borderline-near areas are shear stresses, strain concentrations and ultra-structural feature amplification. Due to the exposed position at the edges of the cell layer with its higher and turbulent fluid flows they are predestinated to occur more often.

---

## **5 Summary and conclusion**

---

To promote stem cell growth the established generally accepted standard in tissue engineering is to mimic physiological conditions in the best possible way. Therefore, the adaption of physiological oxygen concentration needs to be involved in this topic. The work on hand aimed to examine the beneficial influences of cell culture conditions of osteogenically differentiating adMSCs. This examination was conducted with a focus on oxygen, glucose and lactate concentrations.

Both, normoxia and hypoxia revealed mineral accumulation in an early stage beginning with differentiation day seven. Normoxia resulted in stronger and oftentimes earlier mineralization. Concerning this outcome, it should be noted that the number of cell passages performed previous to the cultivation is considered crucial regarding the effect of promoting or inhibiting osteogenesis.

The increased maturation and abnormal findings of borderline-near cell layer areas is traced back to shear stresses, strain concentrations and ultra-structural feature amplification. Also increased cell-cell contacts of cell layer borderlines due to wrapping processes is assumed to have an impact on the increased ossification of these areas.

The used low-glucose medium did not sufficiently supply glucose to nurture hypoxia experiencing adMSCs. In the case of normoxia, where glucose levels were sufficient until differentiation day 12, a visual distinction after staining between high-glucose media adMSCs cannot be made based on the used methods of detection. This implies an equality of both media to promote osteogenic differentiation.

Glucose consumption was monitored to possess cyclic tendencies independent of its concentration. Regarding this cyclic behavior glucose consumption reaches its maximum after medium exchanges and

decreases in the following course. This behavior is assumed to be caused by inhibition effects of accumulating metabolites.

Lactate synthesis was shown to increase over time. Other than expected no inhibition of rising lactate concentrations could be monitored; at least for concentrations up to 125 mg/dL. Tendencies of increasing lactate yield ratios over the course of the experiment are observed as well. Additionally, hypoxia tends to increase lactate yield ratios. Correlations between low LYRs and high glucose consumptions with stronger ossification could be noticed.

The present results relativize the meaning of orthomolecular conditions in stem cell cultures such as glucose and lactate concentrations but highlight the importance of oxygen levels during osteogenic differentiation. As it is shown, the topic concerning the best nurturing conditions for the differentiation of mesenchymal stem cells remains unsettled but possesses potential for improvement. Therefore, it is highly recommended to invest in further growth of the scientific knowledge concerning consequences of varying oxygen concentrations. Further scientific evidence is especially required to determine under what precise circumstances hypoxia promotes or impedes osteogenic differentiation of mesenchymal stem cells.

---

## 6 Appendix

---

### Materials

**Table 1: Consumables and disposables**

| <b>Name</b>                             | <b>Producer</b>              | <b>Purchase order number</b> |
|---|------------------------------|------------------------------|
| 12-well plate                           | TPP                          | 92012                        |
| 15ml tubes, 15ml centrifuge tube        | Corning                      | 430791                       |
| 1ml tubes, Multi-SafeSeal Tubes, nature | Roth                         | 7080-1                       |
| 24-well plate                           | Sarstedt                     | 83.1836                      |
| 50ml tubes - 50ml centrifuge tube       | Corning                      | 430829                       |
| 6-well plate                            | Sarstedt                     | 83.1839                      |
| Collagen matrix - Matristypt            | Dr Suwelack Skin & Heathcare |                              |
| CryoTube Vials, 1.8 ml                  | Thermo Scientific            | 368632                       |
| Pasteur pipette                         | Brand                        | 747720                       |
| Pipette 10 mL                           | greiner bio-one              | 607180                       |
| Pipette 2 mL - Costar Stripette         | Corning incorporated         | 4486                         |
| Pipette 25 mL                           | greiner bio-one              | 760180                       |
| Pipette 5 mL                            | greiner bio-one              | 606180                       |
| Pipette 50 mL                           | greiner bio-one              | 768180                       |
| Pipette tip 0.5–20 µl                   | Brand                        | 702526                       |
| Pipette tip 2–200 µl                    | Brand                        | 712516                       |
| Pipette tip 50–1000 µl                  | Brand                        | 712521                       |
| Sponceram ®                             | Zellwerk                     | 1011052                      |
| Sterile schott flask                    | VWR                          |                              |
| Sterilfilter - Filtropur S02 µm         | Sarstedt                     | 83.1827                      |
| T25 cultivation flasks - PE             | Sarstedt                     | 83.1810.002                  |
| Vented Cap                              |                              |                              |
| T75 cultivation flasks - PE             | Sarstedt                     | 83.1813.002                  |
| Vented Cap                              |                              |                              |

---

**Table 2: Chemicals**

| <b>Name</b>                  | <b>Producer</b>      | <b>Purchase order number / catalog number</b> |
|------------------------------|----------------------|---|
| Accutase StemPro             | Life Technologies    | A1110501                                      |
| Alizarinrot S                | ROTH                 | 0348.2  |
| Calcein                      | Sigma Aldrich        | C0875-5G                                      |
| DAPI                         | Sigma Aldrich        | D8417-1MG                                     |
| Dexamethasone                | Sigma Aldrich        | D4902-25MG                                    |
| DMSO                         | Sigma Aldrich        | D8418-100ML                                   |
| Dulbeccos MEM                | Sigma Aldrich        | D7777-10L                                     |
| Ethanol - 96 %               | AustrAlco            |   |
| Ethanol Rotipuran 99,8 %     | ROTH                 | 9065.1  |
| FKS Fetal Bovine Serum, Gold | PAA Lab Pasching     | CatNr.: A15-151                               |
| Gentamycin                   | PAA Lab Pasching     | CatNr.:P11004                                 |
| Gentamycin                   | PAA                  | P11-004                                       |
| Human Serum                  | Blutbank Linz        |   |
| L-Ascorbat                   | Sigma Aldrich        | A4544-25G                                     |
| MEM alpha                    | Life Technologies    | 12000-063                                     |
| Natriumhydrogencarbonat      | Sigma Aldrich        | 401676-2.5KG                                  |
| NH ChondroDiff               | Miltenyi Biotec GmbH | 130-091-679                                   |
| NH OsteoDiff. Medium         | Miltenyi Biotec GmbH | 130-091-678                                   |
| NKS Newborn Calf Serum       | PAA Lab Pasching     | CatNr.:B15-001                                |
| PBS tablets 10mg/ml          | GIBCO                | 18912-014                                     |
| Penicillin/Streptomycin      | PAA Lab Pasching     | CatNr.:P11-010                                |
| Penicillin/Streptomycin      |                      |   |
| Phosphate buffered saline    | Invitrogen           | 18912-014                                     |
| SDS-solution                 | Sigma Aldrich        | 71736-100ml                                   |
| Silver-nitrate solution (5%) | ROTH                 | N053.1  |
| Trypan-blue solution         | Sigma Aldrich        | T8154   |
| Trypsin                      | SAFC                 | 59418C  |
| β -Glycerophosphate          | Sigma Aldrich        | 50020-100G                                    |

**Table 3: Buffers, solutions & cell culture media**

| <b>Solution</b>        | <b>Composition</b>   |
|------------------------|--|
| Alizarin red solution  | 0,5 % Alizarinrot w/v in ddH <sub>2</sub> O  |
| DAPI-buffer            | 100mM Tris pH 7, 150 mM NaCl, 1 mM CaCl <sub>2</sub> , 0,5 mM, MgCl <sub>2</sub> , 0,1 % Nonident-P <sub>4</sub> O |
| DAPI-stock solution    | 20 mg/ml DAPI in ddH <sub>2</sub> O  |
| Differentiation medium | 0,5 % Gentamycin v/v für alle Differenzierungsmedien   |
| Expansion medium       | 10 % Humanserum w/v, 0,5 % Gentamycin in $\alpha$ - MEM  |
| Hank's buffer I        | 9,5 g/l ddH <sub>2</sub> O   |
| Cryo medium            | 10 % DMSO, 20 % $\alpha$ -MEM, 70 % Humanserum   |
| MTT-stock solution     | 5 mg/ml in PBS   |
| Von Kossa achromatizer | 5 % Na <sub>2</sub> S <sub>2</sub> O <sub>3</sub> w/v in ddH <sub>2</sub> O  |

**Table 4: Equipment & laboratory devices**

| <b>Name</b>              | <b>Producer</b>   | <b>Type &amp; additional information</b> |
|--------------------------|-------------------|--|
| Autoclave                | Thermo Scientific | Varioclave - 500E                        |
| Centrifuge               | Thermo Scientific | HERAEUS - AC017                          |
| Centrifuge               | Eppendorf         | 5702 - AO229221                          |
| Clean bench              | Thermo Scientific | MSC Advantage                            |
| Clean bench              | Thermo Scientific | HERASAFE KS                              |
| Counting chamber         | Brand             |  |
| Deep freezer             | Thermo Scientific | HERAFREEZE BASIC                         |
| Fluoreszent microscope - | Leica             | EL6000                                   |

|                                      |                          |   |
|--------------------------------------|--------------------------|---|
| illuminant                           |                          |   |
| Fluoreszent<br>microscope-<br>camera | Leica                    | DFC42C  |
| Fluoreszent<br>microscopy            | Leica                    | DMIL LED  |
| Incubator                            | Thermo<br>Scientific     | HERACELL - 240i   |
| Incubator                            | Thermoscientific         | Heracell 150i CO <sup>2</sup> Incubator                   |
| Laminar flow hood                    | Thermo<br>scientific     | MSC1  |
| Magnetic stirrer                     | IKA<br>Labortechnik      |   |
| Microscope                           | Leica                    | transmitted light - DMIL LED                              |
| Microscop-Kamera                     | Leica                    | ICC50HD   |
| Nitrogen generator                   | Parker                   |   |
| Nitrogen generator                   | BiosafeMD                | Cryotherm 55121   |
| Peristaltic pump                     | Thermo<br>Scientific     | HERAEUS CD70  |
| Pipettes Research<br>® Plus          | Eppendorf                |   |
| Pump                                 | ISMATEC                  | IPC<br>HighPrecisionMultichannelDispenser<br>ModelISM931C |
| Shaker                               | ELMI                     | Skyline Orbital Shaker                                    |
| Special accuracy<br>weighing machine | Sartorius                | AW-224  |
| Vortexer                             | Scientific<br>Industries | Vortexgenie 2   |
| Water bath                           | GFL                      |   |
| Weighing mashine                     | Sartorius                | AW9202  |

---

## Media

### Used media in the cell culture

Table 5: Used media

| <b>Solution</b>        | <b>Composition</b>   |
|------------------------|--|
| expansion medium       | 10 % human serum, 0,5 % Gentamicin in $\alpha$ MEM   |
| differentiation medium | 10% human serum, 4% Glycerophosphate, 0.5% Gentamicin, 0.125% L-Ascorbic acid and 0.01% Dexamethasone in $\alpha$ MEM                        |
| cryo-medium            | 10 % DMSO, 20 % $\alpha$ -MEM, 70 % human serum  |
| $\alpha$ MEM           | $\alpha$ MEM powder was dissolved together with 2.2 g $\text{NaHCO}_3$ per liter deionized water; afterwards a sterile filtration took place |
| DMEM                   | DMEM powder was dissolved together with 3.7 g $\text{Na}_2\text{CO}_3$ in 1 liter deionized water  |

### Buffers and solutions

Table 6: Buffers and solutions

| <b>Solution</b>                 | <b>Composition</b>  |
|---------------------------------|---|
| alizarin red solution           | 0,5 % Alizarin red w/v in ddH <sub>2</sub> O                    |
| DAPI buffer                     | 100 mM Tris pH 7, 150 mM NaCl, 1 mM $\text{CaCl}_2$ , 0,5 mM    |
| DAPI-parent solution            | 20 mg/ml DAPI in ddH <sub>2</sub> O                             |
| PBS - phosphate buffered saline | 9,5 g/l ddH <sub>2</sub> O                                      |
| von Kossa-developer solution    | 5 % $\text{Na}_2\text{S}_2\text{O}_3$ w/v in ddH <sub>2</sub> O |
| calcein                         | 100 $\mu$ L/mL in ddH <sub>2</sub> O                            |

## **Cell culture**

### **Adipose tissue derived stem cells**

The cells used in this work were adipose derived mesenchymal stem cells (adMSCs). Adipose derived Mesenchymal stem cells are adult multipotent cells that occur naturally in the human body. They are found in umbilical cord, fatty tissue, cartilage, blood, bone marrow and muscle tissue. As multipotent cells they are capable of undergoing the asymmetrical cell division within the same cell line and splitting into one mother cell and one differentiated daughter cell. Due to their mesenchymal heritage, MSCs differentiate into cells that derive from the blastocystic mesoderm as one of the embryonic blastodermic layers. Dependent on the metabolic, cellular and molecular conditions like cell-cell contact, cytokines and growth factors MSCs can differentiate into chondroblasts, adipocytes, osteoblasts, fibroblasts and their descendants as well as into some sort of muscular tissue. MSC are capable of osteogenic differentiation meaning that their descendants can promote bone formation and therefore regeneration and bone repair (Petite et al. 2000; Kon et al. 2000).

## **Handling**

### **Sterile working in the cell culture**

Working in the laboratory was performed sterile in a clean bench of the category II with laminar air flow. The bench itself was cleaned aseptically by the use of ethanol and UV-radiation. Every outer surface that was put in the clean bench was cleaned and washed with hydrous ethanol of 70 %. Media like water and PBS were autoclaved for 30 minutes at 121°C at 1 bar excess pressure; other media were sterile-filtered. Media were heated in a water bath until they reached a temperature of 37°C.

## **Revitalization of cryo-preserved adipose derived MSC's**

The desired cells were taken from the liquid nitrogen freezer and quickly defrosted in the water bath at 37°C. While the cells were totally defrosted but jet cold, 1 mL of cold  $\alpha$ MEM was added. After 2 minutes the suspension was transferred in a 50 mL tube and another 2 mL of cold  $\alpha$ MEM were added. After two minutes incubation at room temperature the suspension was filled up to 10 mL and centrifuged at 300 x g for 5 minutes. The cell supernatant was extracted and the pellet resuspended in cell culture medium.

## **Cell cultivation and differentiation of adMSCs**

The cells were cultivated in cell culture flasks in  $\alpha$ MEM with additional 10% human serum and 0.5% Gentamicin at a temperature of 37°C in an atmosphere consisting of 21% O<sub>2</sub> under normoxic and 5% under hypoxic conditions. If cells were needed for a differentiation under hypoxic conditions, they were extracted from the liquid nitrogen freezer that had also been cultivated preliminary of the cryo-conservation under hypoxic condition. Cells for normoxic differentiation were treated in the same manner. The cells of passage zero were plated in culture flasks with an area of 175 cm<sup>2</sup> in order to proliferate until the cell number reached the aimed amount. Hypoxic lineages were cultivated under hypoxia, normoxic lineages were cultivated under normoxia. The culture medium was changed every other day.

The cells were seeded in 12-well plates with 2 mL medium per well at 8000 cells/cm<sup>2</sup> and split one time before the differentiation sequence started. Medium volume was exchanged totally every 3 days. The cells were cultivated in  $\alpha$ MEM until the cell layer reached a confluence of about

80%. At this point the medium was changed and the wells filled with differentiation medium.

Due to low proliferation rates of hypoxic donor B cells that would not have been sufficient enough to reach the aimed cell amount necessary for the seeding density of 8000 cells/cm<sup>2</sup> a second charge of cryo-preserved adMSC had to be thawed and proliferated in its own cultivation flask in order to get added up later on. This way the aimed confluence could be achieved. Proliferation reached normal values during the further procedure.

The differentiation took place in a self-mixed medium that consisted of αMEM together with 10% human serum, 4% Glycerophosphate, 0.5% Gentamicin, 0.125% L-Ascorbic acid and 0.01% Dexamethasone. The differentiation began when the cell layer reached a confluence level of about 80%. At this point the cell culture medium was removed and replaced with the described differentiation medium.

### **MSC donors**

For the described experiments adipose derived stem cells in passage zero of two different donors were used. The cells were isolated from a male person born in 1949 and from a female person respectively born in 1959. The male derived cells were isolated on January 17<sup>th</sup> 2013 (in the text referred to as donor A) and cryo-preserved on July 17<sup>th</sup>, 2013, the female derived cells were isolated on July 12<sup>th</sup> 2013 and cryo-preserved on January 22<sup>nd</sup>, 2013 (in the text referred to as donor B). The fat derived primary cells in general were received from "Allgemeines Krankenhaus" in Vienna.

## **Splitting cells**

At about 80 % confluence of the cell layer cells were split, which means they were assembled and re-spread over a bigger surface. This needs to be done to inhibit the cells differentiation or even dead that is triggered by the contact inhibition of cells. Therefore the culture medium was removed and the cell layer got washed with PBS and removed from the culture flask surface by means of accutase during 5 minutes incubation at 37°C. The accutase is stopped in its activity by adding one-and-a-half times more culture medium. The cell suspension is then harvested and centrifuged at 300 x g for 5 minutes. The produced cell pellet is flicked and re-suspended in fresh culture medium.

## **Fixation with the use of ethanol**

Before staining cell layers or using fluorescence microscopy in order to state the cells proliferation or ossification stage fixation took place in order to keep the cells in the same condition at the time the cells should be examined. Therefore the cell samples were washed once with PBS and incubated for one hour at 4°C with freezing 96% pure cold ethanol. Afterward the samples were washed three times with PBS cell layers got covered with PBS and stored at 4°C.

## **Histological examination and measurements**

### **Glucose and lactate measurement**

The measurement was performed with the specialized measurement machine Super GL compact manufactured by Hitado with a measurement area of 11-910mg/dL for glucose and 4.5-270mg/dL for lactate with an accuracy of at least 1.5% at 260mg/dL for glucose and 2.0% at 90mg/dL

for lactate. The amount of glucose and lactate is calculated via a biosensor that works enzymatically with calibrating and controlling solutions. The amount of molecules of lactate or glucose is determined by transforming the compounds to gluconic acid or pyruvate respectively. During this reaction two electrons are released for each molecule and measured via a platinum electrode.

To measure the amount of glucose and lactate in the cell culture media 10 $\mu$ L samples are taken by a PIPETBOY pipettor and pipetted in an measurement buffer of 500 $\mu$ L, vortexed and put in the Hitado Super GL compact. When the measurement resulted in extreme values the same solution was measured another time and the average result was noted.

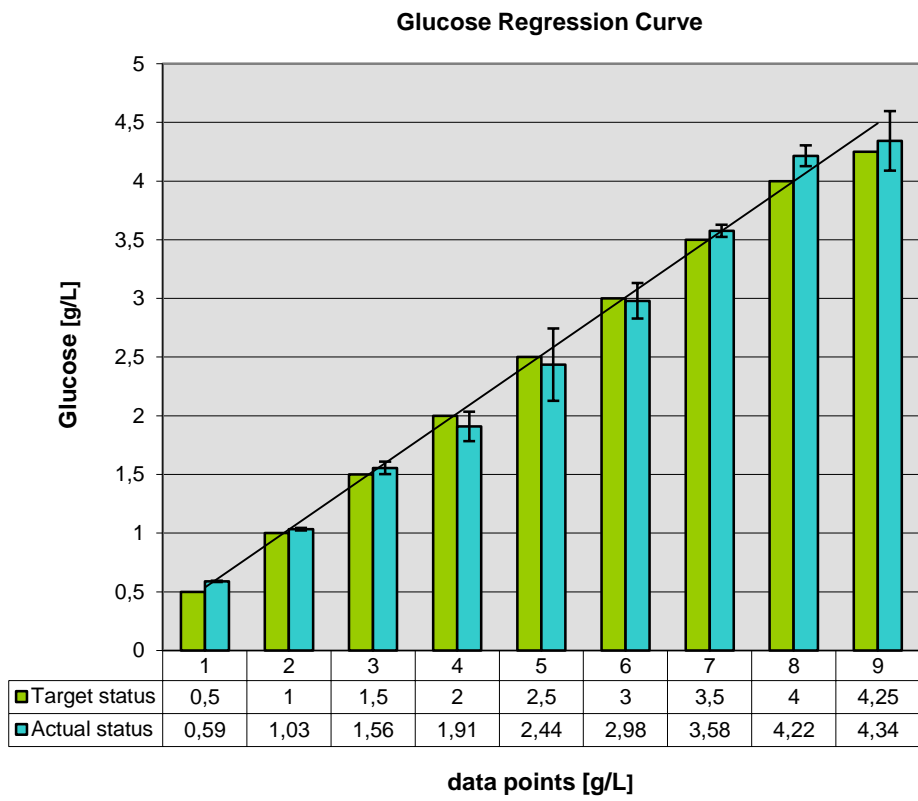


**Figure 23: Error curve for glucose showing the differences between real and measured values**

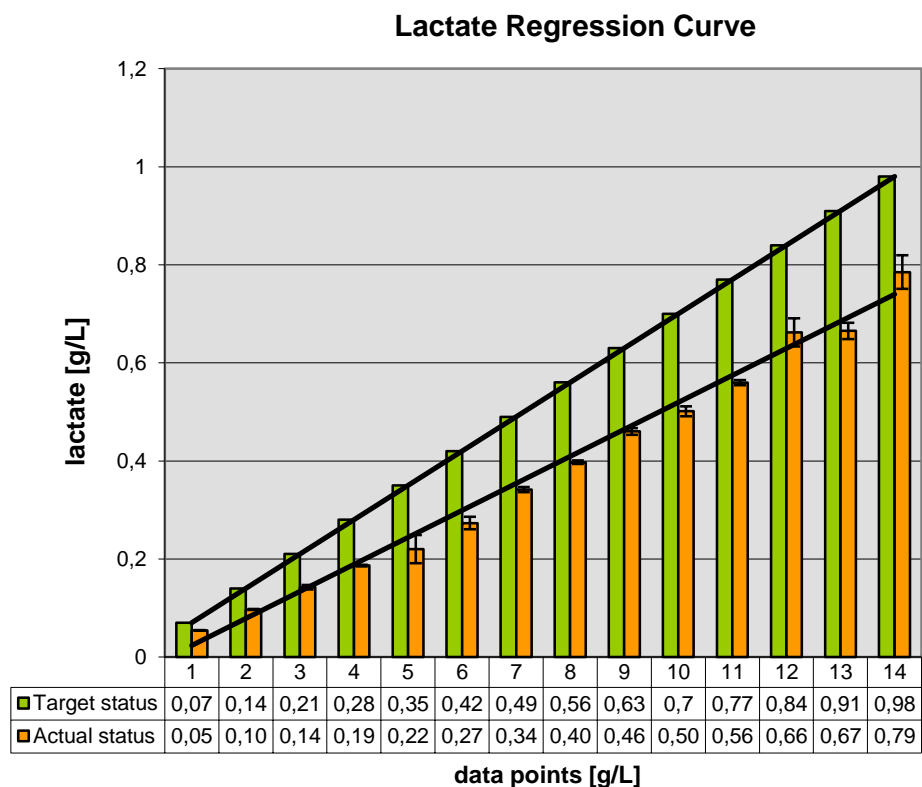


**Figure 24: Error curve for lactate showing differences between real and measured values**

To quantify the systematic error of the measuring machine for glucose and lactate an error curve was established. Therefore mixtures were assembled with specific values of glucose or lactate respectively with a range of 0 – 5 g/L for glucose and 0 – 0.98 g/L for lactate with an increment of 0.5 g/L for glucose and 0.07 g/L for lactate. Each sample was mixed in 1.5 mL tubes from stocks of 1 mg/mL and 10 mg/mL and dissolved in water. Analogous to the measurement procedure of the differentiation medium the measurement of the mixtures was conducted by taking 10  $\mu$ L and adding them to a micro test tube (1.5 mL - Sysmex) filled with 500 $\mu$ L hemolysis buffer. The micro test tube was carefully vortexed and measured twice. Two measurements in a row with one eppi is the limit due to the limited amount of liquid (510  $\mu$ L) in the micro test

tube. The average was taken from the two values either for glucose and lactate for each micro test tube.

Each point on the error curve was replicated four times this way. The resulting values represent the 4 technical replica for each technical sample. The standard deviation resulting from these 4 different samples was computed and used to perform an error curve.

The mathematical formula for the glucose regression curve can be described as:

$$y = 1,0236x - 0,0179 \quad (2)$$

For lactate the regression curve is defined by

$$y = 0,7871x - 0,0313 \quad (3)$$

To transform the measured amount of glucose or lactate respectively into the actual amount of compound one has to compute the inverse function of the functions above and calculate the value for x. The inverse functions are the following:

$$x(y) = 1,27049 \times y(\text{lactate}) + 0,039663 \quad (4)$$

$$x(y) = 0,976944 \times y(\text{glucose}) + 0,0175356 \quad (5)$$

### Cell count determination

To count the number of alive and dead cells Neubauer Counting Chambers with a volume of  $0.1 \text{ mm}^3$  were used. Hereby  $20\mu\text{L}$  of trypan blue was taken and blended with  $20\mu\text{L}$  of a cell suspension. The number of cells was computed with the help of the formula below.

$$\frac{\sum \text{cells in counting quadrates}}{\sum \text{counting quadrates}} \times \text{dilution factor} \times \text{conversion factor in mL}$$

$$= \frac{\sum \text{cells in counting quadrates}}{8} \times 2 \times 10^4 = \frac{\text{Zellzahl}}{\text{mL}} \quad (6)$$

#### Computing the number of cells per mL

### Calcein staining

Calcium accumulation in the extracellular matrix was detected by calcein fluorescent staining. Calcein also known as fluorexon is capable of binding for instance  $\text{Ca}^{2+}$  and  $\text{Mg}^{2+}$  via a coordination complex. The quantity of the resulting coordination complexes can be detected via fluorescence spectrometry with an excitation maximum of 495 nm. This method is used to detect the amount of calcium ions in the extracellular matrix. The samples got washed three times with PBS and were afterwards incubated over night at  $4^\circ\text{C}$  with 1 mL calcein solution that consists of 0.1% of the calcein parent solution solved in PBS. After the incubation the cell layers were washed three times with PBS and the examination was operated.

## **DAPI staining**

With the aid of DAPI staining one can investigate the amount of cells via fluorescence microscopy measured photometrical at the wavelength of maximum absorption of 358 nm. The staining that consists of 4',6-diamidin-2-phenylindol attaches on the DNA strings especially in the minor groove at AT-rich regions.

Fixed cells were washed three times with PBS and incubated at 37°C with a DAPI solution that consists of 0.1% DAPI (parent solution). Afterwards cells were washed three times with PBS before the examination under the fluorescence microscope took place.

## **Alizarin red staining to detect calcium ions**

The accumulation of  $\text{Ca}^{2+}$  ions in the extracellular matrix was detected by alizarin red staining. Alizarin red reacts with  $\text{Ca}^{2+}$  ions by forming a Coordination complex that emits orange / red light. The fixated samples were washed with PBS and afterward incubated with a solution of 0.5% alizarin red for 15 minutes. The samples were washed three times with PBS until the cell layer ceased staining the PBS solution. Afterward the samples got examined via transmitted light microscopy and flat-bed scanner.

## **Von Kossa staining to detect phosphate**

The cell differentiation towards the osteogenic lineage was investigated via von Kossa staining. Von Kossa staining reacts with phosphate in the extracellular matrix derived from calciumphosphate that is the main inorganic component of human bones. Here silver cations get reduced by phosphate to black silver phosphate.

The fixated samples were washed three times with ddH<sub>2</sub>O and afterwards incubated 30 minutes in the dark together with a 5% concentration of AgNO<sub>3</sub> hydrous solution (ddH<sub>2</sub>O). After the incubation the samples were washed thrice and got radiated with UV-light for 2 minutes. After the silver ions got reduced the background was decolorized by adding a developer solution of 5 % concentrated aqueous Na<sub>2</sub>S<sub>2</sub>O<sub>3</sub>. After washing three times with ddH<sub>2</sub>O the staining intensity was documented via transmitting light microscopy and flat-bed scanning.

## Error curve corrected measurement of glucose and lactate

|     |   |       | day 1  |         |          |         | day 2  |         |          |         | day 3  |         |          |         |
|-----|---|-------|--------|---------|----------|---------|--------|---------|----------|---------|--------|---------|----------|---------|
|     |   |       | A      | A       | B        | B       | A      | A       | B        | B       | A      | A       | B        | B       |
|     |   |       | well I | well II | well III | well IV | well I | well II | well III | well IV | well I | well II | well III | well IV |
| Glu | a | ANII  | 76,20  | 73,31   | 71,76    | 72,69   | 47,96  | 53,66   | 52,26    | 50,11   | 66,43  | 37,61   | 42,69    | 32,92   |
| Lac | a |       | 25,18  | 30,27   | 36,24    | 36,62   | 58,03  | 57,01   | 54,91    | 45,89   | 59,11  | 58,85   | 61,52    | 51,48   |
| Glu | d |       | 365,18 | 363,55  | 359,32   | 352,80  | 334,89 | 329,03  | 324,15   | 314,38  | 333,91 | 320,24  | 304,61   | 297,77  |
| Lac | d |       | 32,17  | 35,47   | 36,11    | 39,29   | 49,45  | 47,29   | 53,77    | 57,45   | 70,67  | 68,25   | 73,34    | 77,53   |
| Glu | a | VNII  | 97,45  | 71,70   | 73,27    | 75,90   | 45,03  | 54,90   | 53,34    | 52,07   | 45,03  | 42,69   | 40,93    | 40,83   |
| Lac | a |       | 24,80  | 22,77   | 24,17    | 25,82   | 41,32  | 40,43   | 43,22    | 44,75   | 53,26  | 50,97   | 52,24    | 53,39   |
| Glu | d |       | 363,22 | 369,08  | 361,27   | 357,36  | 352,48 | 338,80  | 336,85   | 333,91  | 328,05 | 309,49  | 294,84   | 294,84  |
| Lac | d |       | 23,79  | 23,66   | 25,95    | 27,09   | 48,31  | 45,38   | 51,10    | 52,50   | 63,17  | 57,58   | 61,14    | 61,14   |
| Glu | a | AHII  | 73,56  | 71,70   | 62,32    | 71,75   | 35,36  | 42,39   | 35,95    | 37,61   | 1,75   | 1,75    | 1,75     | 1,75    |
| Lac | a |       | 27,60  | 22,64   | 21,63    | 26,20   | 66,22  | 63,04   | 72,06    | 72,06   | 111,70 | 107,00  | 113,36   | 115,01  |
| Glu | d |       | 408,16 | 360,29  | 369,08   | 351,50  | 333,91 | 321,21  | 306,56   | 313,40  | 282,14 | 275,30  | 271,39   | 258,69  |
| Lac | d |       | 30,27  | 28,49   | 28,99    | 29,50   | 71,56  | 66,47   | 74,73    | 78,16   | 138,64 | 128,86  | 139,91   | 143,72  |
| Glu | a | VHII  | 92,80  | 73,66   | 72,48    | 70,73   | 33,90  | 43,08   | 35,36    | 40,54   | 1,75   | 19,73   | 15,53    | 18,56   |
| Lac | a |       | 37,63  | 28,23   | 29,63    | 28,23   | 67,49  | 63,43   | 71,94    | 70,92   | 93,79  | 91,38   | 98,24    | 97,86   |
| Glu | d |       | 368,11 | 367,13  | 360,29   | 363,22  | 342,71 | 319,26  | 294,84   | 310,47  | 288,98 | 286,04  | 271,39   | 264,55  |
| Lac | d |       | 30,14  | 28,23   | 29,88    | 30,65   | 69,90  | 67,24   | 72,57    | 80,20   | 118,44 | 118,31  | 115,64   | 123,39  |
| Glu | a | ANIII | 72,48  | 77,27   | 75,02    | 73,95   | 42,79  | 50,31   | 49,53    | 47,38   | 27,54  | 39,76   | 35,95    | 34,87   |
| Lac | a |       | 27,60  | 25,06   | 26,20    | 25,18   | 47,16  | 45,00   | 47,16    | 51,86   | 59,61  | 57,96   | 62,54    | 60,76   |
| Glu | d |       | 376,90 | 366,15  | 367,13   | 372,99  | 328,05 | 334,89  | 330,01   | 317,31  | 312,42 | 318,28  | 312,42   | 285,07  |
| Lac | d |       | 25,06  | 24,17   | 25,56    | 26,96   | 54,15  | 49,70   | 53,13    | 57,20   | 73,08  | 68,76   | 76,13    | 75,75   |
| Glu | a | VNIII | 77,47  | 73,56   | 71,70    | 70,82   | 56,07  | 55,78   | 53,92    | 56,17   | 21,29  | 21,29   | 21,29    | 21,29   |
| Lac | a |       | 26,33  | 25,18   | 25,95    | 28,36   | 47,16  | 42,21   | 44,62    | 44,62   | 67,49  | 67,49   | 67,49    | 67,49   |
| Glu | d |       | 355,41 | 355,41  | 349,55   | 328,05  | 346,61 | 340,75  | 334,89   | 347,59  | 317,31 | 307,54  | 301,68   | 305,58  |
| Lac | d |       | 25,82  | 24,42   | 24,80    | 25,82   | 48,81  | 45,77   | 50,09    | 54,02   | 64,31  | 60,88   | 64,70    | 65,20   |
| Glu | a | AHIII | 62,62  | 73,36   | 71,12    | 73,75   | 43,18  | 40,83   | 33,70    | 33,70   | 1,75   | 1,75    | 1,75     | 1,75    |
| Lac | a |       | 30,65  | 29,88   | 31,66    | 33,95   | 57,07  | 63,43   | 72,32    | 70,92   | 105,61 | 108,40  | 116,02   | 117,04  |
| Glu | d |       | 379,83 | 360,62  | 363,22   | 338,80  | 328,05 | 314,38  | 315,35   | 310,47  | 288,00 | 274,32  | 279,21   | 269,44  |
| Lac | d |       | 31,03  | 25,50   | 33,06    | 31,92   | 68,76  | 67,11   | 78,42    | 78,04   | 142,45 | 131,02  | 144,99   | 139,91  |
| Glu | a | VHIII | 72,58  | 71,90   | 76,39    | 71,90   | 34,48  | 43,27   | 37,12    | 33,41   | 1,75   | 1,75    | 1,75     | 1,75    |
| Lac | a |       | 27,47  | 29,25   | 32,43    | 30,39   | 74,86  | 66,35   | 82,48    | 82,61   | 113,86 | 103,95  | 112,72   | 114,88  |
| Glu | d |       | 366,15 | 355,41  | 361,27   | 364,20  | 361,27 | 319,26  | 334,89   | 301,68  | 291,91 | 259,67  | 252,83   | 243,06  |
| Lac | d |       | 29,38  | 29,38   | 30,77    | 30,77   | 78,04  | 69,78   | 91,88    | 88,33   | 133,56 | 127,08  | 143,72   | 150,07  |

|     |   |       | day 4  |         |          |         | day 5  |         |          |         | day 6  |         |          |         |
|-----|---|-------|--------|---------|----------|---------|--------|---------|----------|---------|--------|---------|----------|---------|
|     |   |       | A      | A       | B        | B       | A      | A       | B        | B       | A      | A       | B        | B       |
|     |   |       | well I | well II | well III | well IV | well I | well II | well III | well IV | well I | well II | well III | well IV |
| Glu | a | ANII  | 61,25  | 62,23   | 58,90    | 64,08   | 47,87  | 35,85   | 35,95    | 41,32   | 32,14  | 35,56   | 23,93    | 27,74   |
| Lac | a |       | 31,92  | 32,93   | 38,78    | 32,17   | 46,91  | 57,20   | 56,31    | 51,23   | 60,25  | 61,39   | 74,35    | 69,27   |
| Glu | d |       | 368,11 | 349,55  | 346,61   | 367,13  | 321,21 | 320,24  | 307,54   | 297,77  | 323,17 | 306,56  | 274,32   | 234,27  |
| Lac | d |       | 34,46  | 36,62   | 46,65    | 46,27   | 54,28  | 59,23   | 81,47    | 78,93   | 77,40  | 79,81   | 119,58   | 110,18  |
| Glu | a | VNII  | 68,97  | 69,65   | 60,27    | 61,35   | 48,16  | 56,66   | 35,95    | 38,19   | 40,34  | 43,57   | 17,29    | 17,78   |
| Lac | a |       | 35,73  | 31,15   | 39,16    | 36,36   | 50,47  | 46,40   | 65,71    | 66,35   | 62,66  | 58,85   | 83,12    | 83,50   |
| Glu | d |       | 335,87 | 344,66  | 334,89   | 334,89  | 342,71 | 326,10  | 307,54   | 315,35  | 330,01 | 315,35  | 275,30   | 283,11  |
| Lac | d |       | 35,86  | 40,43   | 47,80    | 41,95   | 66,73  | 69,02   | 87,82    | 71,94   | 93,28  | 98,36   | 127,71   | 117,17  |
| Glu | a | AHII  | 30,38  | 35,46   | 30,08    | 29,01   | 1,75   | 1,75    | 1,75     | 1,75    | 1,75   | 1,75    | 1,75     | 1,75    |
| Lac | a |       | 72,57  | 70,67   | 77,40    | 79,94   | 108,53 | 107,00  | 110,50   | 107,32  | 120,85 | 121,74  | 116,40   | 116,91  |
| Glu | d |       | 320,24 | 303,63  | 295,81   | 309,49  | 241,10 | 243,06  | 259,67   | 255,76  | 182,49 | 184,44  | 214,73   | 206,91  |
| Lac | d |       | 91,88  | 88,33   | 80,20    | 85,66   | 166,59 | 160,24  | 134,83   | 137,37  | 252,98 | 239,01  | 205,97   | 212,33  |
| Glu | a | VHII  | 29,30  | 38,00   | 32,23    | 35,26   | 1,75   | 1,75    | 1,75     | 1,75    | 1,75   | 1,75    | 1,75     | 1,75    |
| Lac | a |       | 75,88  | 72,32   | 78,42    | 80,58   | 118,44 | 119,20  | 121,11   | 119,58  | 125,30 | 121,11  | 120,85   | 121,99  |
| Glu | d |       | 317,31 | 305,58  | 305,58   | 300,70  | 261,62 | 244,04  | 256,74   | 251,85  | 217,66 | 207,89  | 222,54   | 209,84  |
| Lac | d |       | 80,45  | 84,01   | 83,24    | 84,26   | 161,51 | 164,05  | 153,88   | 158,97  | 241,55 | 244,09  | 223,76   | 231,38  |
| Glu | a | ANIII | 63,98  | 65,94   | 63,11    | 64,08   | 43,18  | 47,47   | 33,90    | 34,09   | 27,74  | 34,68   | 20,61    | 18,90   |
| Lac | a |       | 30,65  | 29,88   | 31,03    | 31,66   | 46,02  | 45,64   | 59,74    | 57,45   | 61,14  | 60,12   | 78,54    | 79,05   |
| Glu | d |       | 363,22 | 365,18  | 348,57   | 343,68  | 324,15 | 318,28  | 303,63   | 305,58  | 304,61 | 291,91  | 259,67   | 266,51  |
| Lac | d |       | 37,00  | 37,89   | 39,03    | 38,27   | 63,55  | 63,04   | 76,38    | 73,59   | 89,85  | 87,56   | 116,91   | 117,55  |
| Glu | a | VNIII | 58,03  | 65,65   | 59,30    | 67,21   | 52,75  | 53,04   | 33,99    | 44,84   | 46,99  | 36,34   | 14,75    | 19,53   |
| Lac | a |       | 29,25  | 30,77   | 38,14    | 32,81   | 42,59  | 49,20   | 66,16    | 57,84   | 54,53  | 63,04   | 83,75    | 72,70   |
| Glu | d |       | 370,06 | 332,94  | 329,03   | 338,80  | 352,48 | 330,01  | 297,77   | 305,58  | 359,32 | 317,31  | 274,32   | 275,30  |
| Lac | d |       | 32,55  | 36,49   | 45,38    | 43,86   | 53,77  | 64,95   | 86,68    | 86,42   | 74,86  | 91,25   | 130,38   | 132,29  |
| Glu | a | AHIII | 32,58  | 37,12   | 32,53    | 32,23   | 1,75   | 1,75    | 1,75     | 1,75    | 1,75   | 1,75    | 1,75     | 1,75    |
| Lac | a |       | 72,13  | 69,02   | 76,00    | 80,20   | 113,23 | 112,85  | 112,72   | 114,12  | 120,85 | 115,26  | 116,40   | 119,20  |
| Glu | d |       | 331,96 | 308,51  | 312,42   | 317,31  | 240,13 | 244,04  | 261,62   | 256,74  | 193,23 | 196,17  | 225,47   | 220,59  |
| Lac | d |       | 91,38  | 89,85   | 80,83    | 83,88   | 165,32 | 167,86  | 144,99   | 146,26  | 252,98 | 240,28  | 211,06   | 217,41  |
| Glu | a | VHIII | 31,45  | 38,78   | 30,96    | 32,14   | 1,75   | 1,75    | 1,75     | 1,75    | 1,75   | 1,75    | 1,75     | 1,75    |
| Lac | a |       | 74,86  | 74,48   | 82,36    | 83,24   | 121,49 | 117,80  | 119,07   | 118,44  | 123,52 | 123,39  | 121,23   | 120,60  |
| Glu | d |       | 320,24 | 307,54  | 310,47   | 313,40  | 245,01 | 238,17  | 260,64   | 249,90  | 197,14 | 190,30  | 209,84   | 205,93  |
| Lac | d |       | 93,03  | 95,70   | 86,42    | 86,17   | 175,48 | 180,56  | 158,97   | 156,43  | 256,79 | 255,52  | 217,41   | 221,22  |

|     |   | day 7  |         |          |         | day 8  |         |          |         | day 9  |         |          |         |        |
|-----|---|--------|---------|----------|---------|--------|---------|----------|---------|--------|---------|----------|---------|--------|
|     |   | A      | A       | B        | B       | A      | A       | B        | B       | A      | A       | B        | B       |        |
|     |   | well I | well II | well III | well IV | well I | well II | well III | well IV | well I | well II | well III | well IV |        |
| Glu | a | ANII   | 61,54   | 67,50    | 60,86   | 59,88  |         |          |         |        |         |          |         |        |
| Lac | a |        | 42,97   | 42,46    | 50,72   | 52,24  |         |          |         |        |         |          |         |        |
| Glu | D |        | 369,08  | 351,50   | 324,15  | 315,35 |         |          |         |        |         |          |         |        |
| Lac | D |        | 48,94   | 52,24    | 81,97   | 83,75  |         |          |         |        |         |          |         |        |
| Glu | a | VNII   | 62,03   | 67,60    | 53,24   | 66,82  |         |          |         |        |         |          |         |        |
| Lac | a |        | 42,08   | 44,24    | 61,90   | 50,85  |         |          |         |        |         |          |         |        |
| Glu | D |        | 354,43  | 347,59   | 348,57  | 335,87 |         |          |         |        |         |          |         |        |
| Lac | D |        | 53,52   | 57,20    | 80,83   | 95,19  |         |          |         |        |         |          |         |        |
| Glu | a | AHII   | 18,07   | 35,17    | 17,09   | 21,19  |         |          |         |        |         |          |         |        |
| Lac | a |        | 89,47   | 79,69    | 104,72  | 99,38  |         |          |         |        |         |          |         |        |
| Glu | D |        | 365,18  | 314,38   | 295,81  | 297,77 |         |          |         |        |         |          |         |        |
| Lac | D |        | 61,01   | 99,76    | 110,69  | 112,59 |         |          |         |        |         |          |         |        |
| Glu | a | VHII   | 9,57    | 36,34    | 12,60   | 16,21  |         |          |         |        |         |          |         |        |
| Lac | a |        | 103,06  | 82,99    | 102,05  | 105,73 |         |          |         |        |         |          |         |        |
| Glu | D |        | 300,70  | 303,63   | 285,07  | 282,14 |         |          |         |        |         |          |         |        |
| Lac | D |        | 124,54  | 116,53   | 123,77  | 127,33 |         |          |         |        |         |          |         |        |
| Glu | a | ANIII  | 56,27   | 64,47    | 53,73   | 67,40  | 6,47    | 6,11     | 16,75   | 6,02   | 29,99   | 27,54    | 1,75    | 30,48  |
| Lac | a |        | 40,05   | 41,57    | 55,80   | 45,89  | 63,81   | 63,43    | 91,57   | 70,54  | 78,54   | 78,67    | 106,62  | 87,06  |
| Glu | D |        | 371,04  | 343,68   | 319,26  | 315,35 | 327,08  | 306,56   | 287,02  | 254,78 | 289,95  | 278,23   | 222,54  | 197,14 |
| Lac | D |        | 62,03   | 59,49    | 83,50   | 91,38  | 110,94  | 109,93   | 166,59  | 175,48 | 146,26  | 143,72   | 231,38  | 240,28 |
| Glu | a | VNIII  | 60,66   | 64,08    | 49,04   | 53,92  | 35,17   | 35,95    | 7,37    | 19,14  | 22,56   | 25,20    | 1,75    | 1,75   |
| Lac | a |        | 40,68   | 45,26    | 62,41   | 59,36  | 65,59   | 62,79    | 97,86   | 88,33  | 85,28   | 89,34    | 116,02  | 111,96 |
| Glu | D |        | 377,88  | 344,66   | 328,05  | 318,28 | 325,12  | 292,88   | 250,87  | 252,83 | 290,93  | 258,69   | 210,82  | 213,75 |
| Lac | D |        | 44,24   | 58,85    | 87,44   | 90,61  | 91,88   | 111,58   | 160,24  | 161,51 | 138,64  | 155,15   | 222,49  | 246,63 |
| Glu | a | AHIII  | 22,27   | 36,34    | 28,13   | 17,29  | 1,75    | 1,75     | 1,75    | 1,75   | 1,75    | 1,75     | 1,75    | 1,75   |
| Lac | a |        | 89,85   | 75,05    | 105,22  | 102,94 | 128,86  | 123,01   | 127,97  | 124,66 | 134,83  | 133,56   | 127,33  | 128,47 |
| Glu | D |        | 315,35  | 340,75   | 306,56  | 297,77 | 231,34  | 316,33   | 224,50  | 225,47 | 182,49  | 291,42   | 184,44  | 184,44 |
| Lac | D |        | 107,51  | 63,43    | 115,39  | 115,64 | 212,33  | 107,96   | 208,52  | 208,52 | 292,37  | 144,99   | 292,37  | 297,45 |
| Glu | a | VHIII  | 24,61   | 36,34    | 19,34   | 18,46  | 1,75    | 1,75     | 1,75    | 1,75   | 1,75    | 1,75     | 1,75    | 1,75   |
| Lac | a |        | 92,52   | 82,36    | 102,05  | 105,86 | 124,28  | 120,72   | 121,99  | 125,30 | 131,02  | 127,46   | 123,27  | 122,76 |
| Glu | D |        | 304,61  | 290,93   | 299,72  | 288,00 | 240,13  | 215,70   | 252,83  | 213,75 | 185,42  | 165,88   | 181,51  | 161,97 |
| Lac | D |        | 109,67  | 114,75   | 113,36  | 127,33 | 212,33  | 216,14   | 207,24  | 223,76 | 287,29  | 297,45   | 270,77  | 296,18 |

|     |   | day 10 |         |          |         | day 11 |         |          |         | day 12 |         |          |         |        |
|-----|---|--------|---------|----------|---------|--------|---------|----------|---------|--------|---------|----------|---------|--------|
|     |   | well I | well II | well III | well IV | well I | well II | well III | well IV | well I | well II | well III | well IV |        |
| Glu | a | ANIII  | 1,75    | 12,50    | 1,75    | 24,52  | 63,89   | 55,49    | 39,85   | 61,54  | 33,50   | 33,31    | 1,75    | 53,53  |
| Lac | a |        | 112,72  | 107,89   | 123,65  | 96,20  | 48,18   | 52,50    | 64,95   | 34,71  | 85,02   | 83,75    | 119,07  | 71,30  |
| Glu | D |        | 285,07  | 303,63   | 243,06  | 241,10 | 372,99  | 367,13   | 330,98  | 330,98 | 351,50  | 354,43   | 324,15  | 327,08 |
| Lac | D |        | 175,48  | 169,13   | 204,70  | 207,24 | 75,24   | 73,84    | 78,10   | 49,07  | 134,83  | 129,49   | 164,05  | 172,94 |
| Glu | a | VNIII  | 1,75    | 1,75     | 1,75    | 1,75   | 47,96   | 62,32    | 46,50   | 45,72  | 28,33   | 30,67    | 1,75    | 1,75   |
| Lac | a |        | 102,94  | 97,09    | 106,37  | 104,21 | 49,96   | 45,38    | 62,15   | 54,79  | 82,86   | 78,80    | 104,14  | 113,55 |
| Glu | D |        | 261,62  | 251,85   | 254,78  | 227,43 | 347,59  | 318,28   | 345,64  | 343,68 | 312,42  | 302,65   | 292,88  | 279,21 |
| Lac | D |        | 174,21  | 156,43   | 183,11  | 183,11 | 72,45   | 67,87    | 71,30   | 67,49  | 132,29  | 125,30   | 132,29  | 136,10 |
| Glu | a | AHIII  | 1,75    | 1,75     | 1,75    | 1,75   | 13,87   | 33,31    | 1,75    | 1,75   | 1,75    | 1,75     | 1,75    | 1,75   |
| Lac | a |        | 136,10  | 134,83   | 130,51  | 134,83 | 65,71   | 79,24    | 88,84   | 69,27  | 127,46  | 128,35   | 132,29  | 125,81 |
| Glu | D |        | 290,93  | 285,07   | 148,30  | 137,55 | 357,36  | 344,66   | 281,16  | 283,11 | 345,64  | 328,05   | 219,61  | 223,52 |
| Lac | D |        | 160,24  | 176,75   | 324,13  | 345,73 | 61,39   | 53,52    | 123,90  | 123,77 | 112,08  | 112,85   | 226,30  | 235,20 |
| Glu | a | VHIII  | 1,75    | 1,75     | 1,75    | 1,75   | 14,55   | 30,08    | 17,19   | 21,29  | 1,75    | 1,75     | 1,75    | 1,75   |
| Lac | a |        | 132,29  | 132,29   | 127,58  | 131,02 | 89,98   | 82,23    | 96,46   | 117,04 | 125,81  | 124,15   | 124,41  | 126,31 |
| Glu | D |        | 227,92  | 289,46   | 157,09  | 160,02 | 320,24  | 336,85   | 289,95  | 275,30 | 289,95  | 322,19   | 229,38  | 232,31 |
| Lac | D |        | 207,88  | 150,71   | 335,56  | 347,00 | 94,55   | 64,95    | 116,40  | 92,90  | 160,24  | 110,43   | 223,76  | 223,76 |

---

## Publication bibliography

---

Abbiss, Chris R.; Laursen, Paul B. (2005): Models to explain fatigue during prolonged endurance cycling. In *Sports medicine* 35 (10), pp. 865–898.

Abdollahi, Hamid; Harris, Lisa J.; Zhang, Ping; McIlhenny, Stephen; Srinivas, Vikram; Tulenko, Thomas; DiMuzio, Paul J. (2011): The role of hypoxia in stem cell differentiation and therapeutics. In *Journal of Surgical Research* 165 (1), pp. 112–117.

Aubin, Jane E.; Triffitt, James T. (2002): Mesenchymal stem cells and osteoblast differentiation. In *Principles of bone biology* 1, pp. 59–81.

Basciano, Leticia; Nemos, Christophe; Foliguet, Bernard; Isla, Natalia de; Carvalho, Marcelo de; Tran, Nguyen; Dalloul, Ali (2011): Long term culture of mesenchymal stem cells in hypoxia promotes a genetic program maintaining their undifferentiated and multipotent status. In *BMC cell biology* 12 (1), p. 12.

Borle, André B.; Nichols, Nancy; Nichols, George (1960): Metabolic studies of bone in vitro II. The metabolic patterns of accretion and resorption. In *Journal of Biological Chemistry* 235 (4), pp. 1211–1214.

Brand, KARL A.; Hermfisse, Ulrich (1997): Aerobic glycolysis by proliferating cells: a protective strategy against reactive oxygen species. In *The FASEB journal* 11 (5), pp. 388–395.

Chen, Ting; Zhou, Yan; Tan, Wen-Song (2009): Influence of lactic acid on the proliferation, metabolism, and differentiation of rabbit mesenchymal stem cells. In *Cell biology and toxicology* 25 (6), pp. 573–586.

Cipolleschi, Maria Grazia; Sbarba, P. Dello; Olivotto, M. (1993): The role of hypoxia in the maintenance of hematopoietic stem cells. In *Blood* 82 (7), pp. 2031–2037.

Coan, Heather Adeline Bradbury (2011): Adipose-Derived Stem Cell Osteogenic Differentiation: A Study of the Influence of Extracellular Matrix on the Differentiation Process.

Cowin, Stephen C. (2001): Bone mechanics handbook.

Cowin, Stephen C.; Doty, Stephen B. (Eds.) (2007): Tissue mechanics. New York, NY: Springer.

Csete, Marie (2005): Oxygen in the cultivation of stem cells. In *Annals of the New York Academy of Sciences* 1049 (1), pp. 1–8.

Dawson, R. M. (1959): C, Elliott, D. C, Elliott, WH, Jones, KM: Data for Biochemical Research: Oxford University Press, London.

Deschepper, M.; Oudina, K.; David, B.; Myrtil, V.; Collet, C.; Bensidhoum, M. et al. (2011): Survival and function of mesenchymal stem cells (MSCs) depend on glucose to overcome exposure to long-term, severe and continuous hypoxia. In *Journal of Cellular and Molecular Medicine* 15 (7), pp. 1505–1514. DOI: 10.1111/j.1582-4934.2010.01138.x.

D'Ippolito, Gianluca; Diabira, Sylma; Howard, Guy A.; Roos, Bernard A.; Schiller, Paul C. (2006): Low oxygen tension inhibits osteogenic differentiation and enhances stemness of human MIAMI cells. In *Bone* 39 (3), pp. 513–522. DOI: 10.1016/j.bone.2006.02.061.

Ezashi, Toshihiko; Das, Padmalaya; Roberts, R. Michael (2005): Low O<sub>2</sub> tensions and the prevention of differentiation of hES cells. In *Proceedings of the National Academy of Sciences of the United States of America* 102 (13), pp. 4783–4788.

Felig (1970): Amino acid metabolism in the regulation of gluconeogenesis in man. In *The American journal of clinical nutrition* 23 (7), pp. 986–992.

Fritton, Susannah P.; J. McLeod, Kenneth; Rubin, Clinton T. (2000): Quantifying the strain history of bone: spatial uniformity and self-similarity of low-magnitude strains. In *Journal of Biomechanics* 33 (3), pp. 317–325. DOI: 10.1016/S0021-9290(99)00210-9.

Fritton, Susannah P.; Weinbaum, Sheldon (2009): Fluid and Solute Transport in Bone: Flow-Induced Mechanotransduction. In *Annu. Rev. Fluid Mech.* 41 (1), pp. 347–374. DOI: 10.1146/annurev.fluid.010908.165136.

Grayson, Warren L.; Zhao, Feng; Bunnell, Bruce; Ma, Teng (2007): Hypoxia enhances proliferation and tissue formation of human mesenchymal stem cells. In *Biochemical and biophysical research communications* 358 (3), pp. 948–953.

Grayson, Warren L.; Zhao, Feng; Izadpanah, Reza; Bunnell, Bruce; Ma, Teng (2006): Effects of hypoxia on human mesenchymal stem cell expansion and plasticity in 3D constructs. In *J. Cell. Physiol.* 207 (2), pp. 331–339. DOI: 10.1002/jcp.20571.

Guillemin, Karen; Krasnow, Mark A. (1997): The hypoxic response: huffing and HIFing. In *Cell* 89 (1), pp. 9–12.

Hassell, T.; Gleave, S.; Butler, M. (1991): Growth inhibition in animal cell culture. In *Applied biochemistry and biotechnology* 30 (1), pp. 29–41.

He, Yao; Wang, WeiRan; Ding, JianDong (2013): Effects of L-lactic acid and D,L-lactic acid on viability and osteogenic differentiation of mesenchymal stem cells. In *Chin. Sci. Bull.* 58 (20), pp. 2404–2411. DOI: 10.1007/s11434-013-5798-y.

Hevehan, Diane L.; De Bernardez Clark, Eliana (1997): Oxidative renaturation of lysozyme at high concentrations. In *Biotechnology and bioengineering* 54 (3), pp. 221–230.

Hevehan, Diane L.; Papoutsakis, E. Terry; Miller, William M. (2000): Physiologically significant effects of pH and oxygen tension on granulopoiesis. In *Experimental hematology* 28 (3), pp. 267–275.

Hoshiba, Takashi; Kawazoe, Naoki; Tateishi, Tetsuya; Chen, Guoping (2009): Development of stepwise osteogenesis-mimicking matrices for the regulation of mesenchymal stem cell functions. In *Journal of Biological Chemistry* 284 (45), pp. 31164–31173.

Jaiswal, Neelam; Haynesworth, Stephen E.; Caplan, Arnold I.; Bruder, Scott P. (1997): Osteogenic differentiation of purified, culture-expanded human mesenchymal stem cells in vitro. In *Journal of cellular biochemistry* 64 (2), pp. 295–312.

Kaysinger, Kathleen K.; Ramp, Warren K. (1998): Extracellular pH modulates the activity of cultured human osteoblasts. In *Journal of cellular biochemistry* 68 (1), pp. 83–89.

Keith, Brian; Simon, M. Celeste (2007): Hypoxia-inducible factors, stem cells, and cancer. In *Cell* 129 (3), pp. 465–472.

Kon, E.; Muraglia, A.; Corsi, A.; Bianco, P.; Marcacci, Mm; Martin, I. et al. (2000): Autologous bone marrow stromal cells loaded onto porous hydroxyapatite ceramic accelerate bone repair in critical-size defects of sheep long bones. In *Journal of biomedical materials research* 49 (3), pp. 328–337.

Krebs, H. A.; Bellamy, D. (1960): The interconversion of glutamic acid and aspartic acid in respiring tissues. In *Biochemical Journal* 75 (3), p. 523.

Langenbach, Fabian; Handschel, Jörg (2013): Effects of dexamethasone, ascorbic acid and  $\beta$ -glycerophosphate on the osteogenic differentiation of stem cells in vitro. In *Stem Cell Res Ther* 4, p. 117.

Lao, Mio-Sam; Toth, Derek (1997): Effects of ammonium and lactate on growth and metabolism of a recombinant Chinese hamster ovary cell culture. In *Biotechnology progress* 13 (5), pp. 688–691.

Liu, Chao; Zhao, Yan; Cheung, Wing-Yee; Gandhi, Ronak; Wang, Liyun; You, Lidan (2010): Effects of cyclic hydraulic pressure on osteocytes. In *Bone* 46 (5), pp. 1449–1456. DOI: 10.1016/j.bone.2010.02.006.

Malhotra, Ricky; Brosius, Frank C. (1999): Glucose uptake and glycolysis reduce hypoxia-induced apoptosis in cultured neonatal rat cardiac myocytes. In *Journal of Biological Chemistry* 274 (18), pp. 12567–12575.

Malladi, Preeti; Xu, Yue; Chiou, Michael; Giaccia, Amato J.; Longaker, Michael T. (2006): Effect of reduced oxygen tension on chondrogenesis and osteogenesis in adipose-derived mesenchymal cells. In *American Journal of Physiology-Cell Physiology* 290 (4), pp. C1139-C1146.

Malone, A. M. D.; Anderson, C. T.; Tummala, P.; Kwon, R. Y.; Johnston, T. R.; Stearns, T.; Jacobs, C. R. (2007): Primary cilia mediate mechanosensing in bone cells by a calcium-independent mechanism. In *Proceedings of the National Academy of Sciences* 104 (33), pp. 13325–13330. DOI: 10.1073/pnas.0700636104.

McCall, Anthony L.; Millington, William R.; Wurtman, Richard J. (1982): Metabolic fuel and amino acid transport into the brain in experimental diabetes mellitus. In *Proceedings of the National Academy of Sciences* 79 (17), pp. 5406–5410.

McKeehan, W. (1982): Glycolysis, glutaminolysis and cell proliferation. In *Cell Biology International Reports* 6 (7), pp. 635–650. DOI: 10.1016/0309-1651(82)90125-4.

McNamara, L. M.; van der Linden, J. C.; Weinans, H.; Prendergast, P. J. (2006): Stress-concentrating effect of resorption lacunae in trabecular

bone. In *Journal of Biomechanics* 39 (4), pp. 734–741. DOI: 10.1016/j.jbiomech.2004.12.027.

Müller, Benjamin; Prante, Christian; Gastens, Martin; Kuhn, Joachim; Kleesiek, Knut; Götting, Christian (2008): Increased levels of xylosyltransferase I correlate with the mineralization of the extracellular matrix during osteogenic differentiation of mesenchymal stem cells. In *Matrix Biology* 27 (2), pp. 139–149.

Nicolella, Daniel P.; Moravits, Donald E.; Gale, Adrian M.; Bonewald, Lynda F.; Lankford, James (2006): Osteocyte lacunae tissue strain in cortical bone. In *Journal of Biomechanics* 39 (9), pp. 1735–1743. DOI: 10.1016/j.jbiomech.2005.04.032.

Nicoll, Steven B.; Wedrychowska, Anna; Smith, Nancy R.; Bhatnagar, Rajendra S. (2001): Modulation of proteoglycan and collagen profiles in human dermal fibroblasts by high density micromass culture and treatment with lactic acid suggests change to a chondrogenic phenotype. In *Connective tissue research* 42 (1), pp. 59–69.

Omasa, Takeshi; Higashiyama, Ken-Ichi; Shioya, Suteaki; Suga, Ken-ichi (1992): Effects of lactate concentration on hybridoma culture in lactate-controlled fed-batch operation. In *Biotechnology and bioengineering* 39 (5), pp. 556–564.

Owen, Thomas A.; Aronow, Michael; Shalhoub, Victoria; Barone, Leesa M.; Wilming, Laurens; Tassinari, Melissa S. et al. (1990): Progressive development of the rat osteoblast phenotype in vitro: Reciprocal relationships in expression of genes associated with osteoblast proliferation and differentiation during formation of the bone extracellular matrix. In *J. Cell. Physiol.* 143 (3), pp. 420–430. DOI: 10.1002/jcp.1041430304.

Ozturk, Sadettin S.; Palsson, Bernhard O. (1991): Effect of medium osmolarity on hybridoma growth, metabolism, and antibody production. In *Biotechnology and bioengineering* 37 (10), pp. 989–993.

Ozturk, Sadettin S.; Riley, Mark R.; Palsson, Bernhard O. (1992): Effects of ammonia and lactate on hybridoma growth, metabolism, and antibody production. In *Biotechnology and bioengineering* 39 (4), pp. 418–431.

Patel, Sanjay D.; Papoutsakis, Eleftherios T.; Winter, Jane N.; Miller, William M. (2000): The lactate issue revisited: novel feeding protocols to examine inhibition of cell proliferation and glucose metabolism in hematopoietic cell cultures. In *Biotechnology progress* 16 (5), pp. 885–892.

Petite, Herve; Viateau, Veronique; Bensaid, Wassila; Meunier, Alain; Pollak, Cindy de; Bourguignon, Marianne et al. (2000): Tissue-engineered bone regeneration. In *Nature biotechnology* 18 (9), pp. 959–963.

Poor, P. R. (2003): The molecular machinery of Keilin's respiratory chain. In *Biochemical Society Transactions* 31 (Pt 6), pp. 1095–1105. DOI: 10.1042/BST0311095.

Prasad, S. M.; Czepiel, M.; Cetinkaya, Cihan; Smigielska, K.; Weli, Simon C.; Lysdahl, Helle et al. (2009): Continuous hypoxic culturing maintains activation of Notch and allows long-term propagation of human embryonic stem cells without spontaneous differentiation. In *Cell proliferation* 42 (1), pp. 63–74.

Rawlinson, S. C. F.; Pitsillides, A. A.; Lanyon, L. E. (1996): Involvement of different ion channels in osteoblasts' and osteocytes' early responses to mechanical strain. In *Bone* 19 (6), pp. 609–614. DOI: 10.1016/S8756-3282(96)00260-8.

Seagroves, Tiffany N.; Ryan, Heather E.; Lu, Han; Wouters, Bradley G.; Knapp, Merrill; Thibault, Pierre et al. (2001): Transcription factor HIF-1 is a necessary mediator of the pasteur effect in mammalian cells. In *Molecular and cellular biology* 21 (10), pp. 3436–3444.

Studer, Lorenz; Csete, Marie; Lee, Sang-Hun; Kabbani, Nadine; Walikonis, Jean; Wold, Barbara; McKay, Ron (2000): Enhanced proliferation, survival, and dopaminergic differentiation of CNS precursors in lowered oxygen. In *The Journal of Neuroscience* 20 (19), pp. 7377–7383.

Vogel, Viola; Sheetz, Michael (2006): Local force and geometry sensing regulate cell functions. In *Nat Rev Mol Cell Biol* 7 (4), pp. 265–275. DOI: 10.1038/nrm1890.

Wang, David W.; Fermor, Beverley; Gimble, Jeffrey M.; Awad, Hani A.; Guilak, Farshid (2005): Influence of oxygen on the proliferation and metabolism of adipose derived adult stem cells. In *Journal of cellular physiology* 204 (1), pp. 184–191.

Wang, Y.; McNamara, L. M.; Schaffler, M. B.; Weinbaum, S. (2007): A model for the role of integrins in flow induced mechanotransduction in osteocytes. In *Proceedings of the National Academy of Sciences* 104 (40), pp. 15941–15946. DOI: 10.1073/pnas.0707246104.

Weatherby, Dicken; Ferguson, Scott (2004): Blood Chemistry and CBC Analysis: Weatherby & Associates, LLC.

Weinbaum, Sheldon; Cowin, Stephen C.; Zeng Y.: A model for the excitation of osteocytes by mechanical loading-induced bone fluid shear stresses. In *Journal of Biomechanics* 1994 (27), pp. 339–360.

Xie, Liqin; Jacobson, Jeffrey M.; Choi, Edna S.; Busa, Bhavin; Donahue, Leah Rae; Miller, Lisa M. et al. (2006): Low-level mechanical vibrations

can influence bone resorption and bone formation in the growing skeleton. In *Bone* 39 (5), pp. 1059–1066. DOI: 10.1016/j.bone.2006.05.012.

Xiong J.; Onal M.; Jilka R.L.; Weinstein R.S.; Manolagas S.C.; O'Brien C.A. (2011): Matrix-embedded cells control osteoclast formation. In *Nature Medicine* (17), pp. 1235–1241.

Xu, Ren; Boudreau, Aaron; Bissell, Mina J. (2009): Tissue architecture and function: dynamic reciprocity via extra-and intra-cellular matrices. In *Cancer and metastasis reviews* 28 (1-2), pp. 167–176.

You, J.; Yellowley, C. E.; Donahue, H. J.; Zhang, Y.; Chen, Q.; Jacobs, C. R. (2000): Substrate Deformation Levels Associated With Routine Physical Activity Are Less Stimulatory to Bone Cells Relative to Loading-Induced Oscillatory Fluid Flow. In *J. Biomech. Eng.* 122 (4), p. 387. DOI: 10.1115/1.1287161.